iScience

CellPress
OPEN ACCESS

Article

Influenza-A mediated pre-existing immunity levels to SARS-CoV-2 could predict early COVID-19 outbreak dynamics

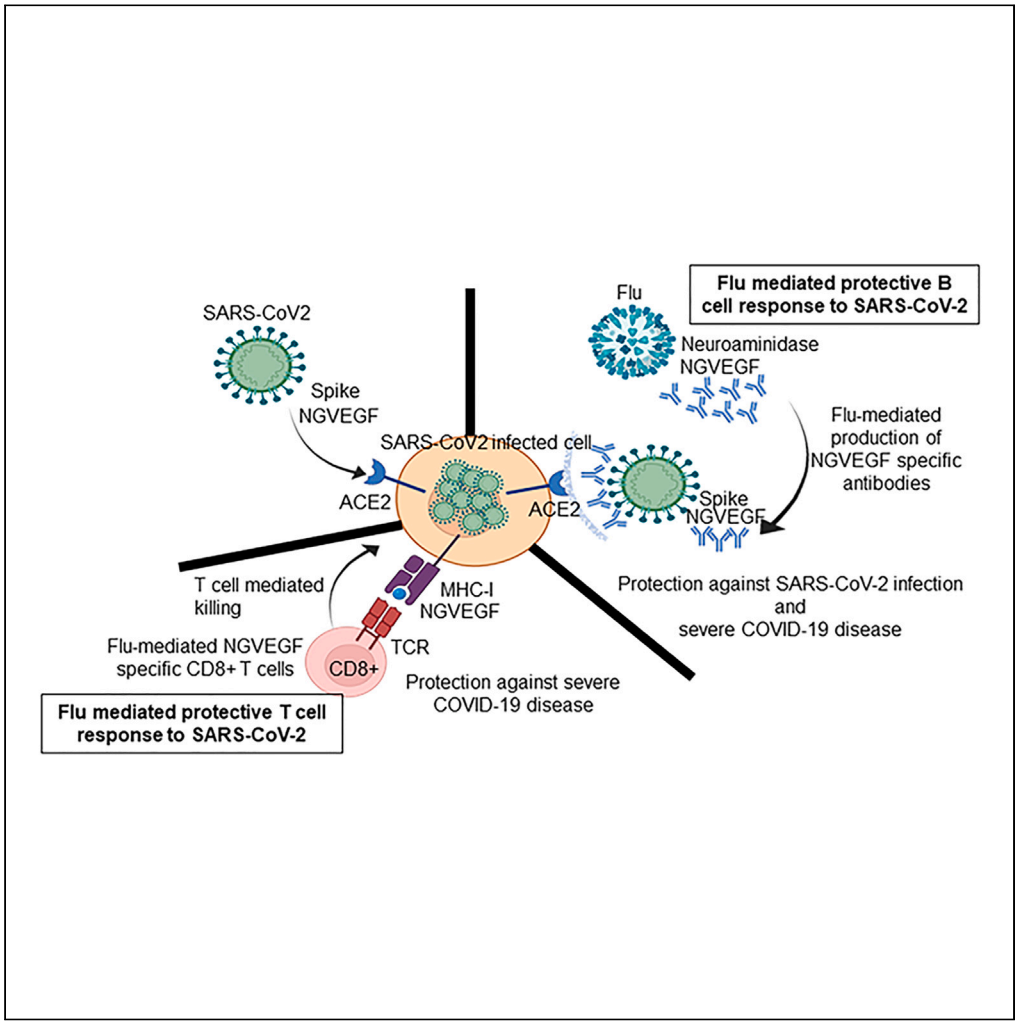

Nerea Martín Almazán, Afsar Rahbar, Marcus Carlsson, ..., Andres Susrud, Birger Sörensen, Cecilia Söderberg-Nauclér

afsar.rahbar@ki.se (A.R.)
cecilia.naucler@ki.se (C.S.-N.)

Highlights

SARS-CoV-2 susceptibility is influenced by a cross-immunity to influenza A H1N1

A common peptide, NGVEGF, provides cross-immunity between FLU strains and SARS-CoV-2

Flu-mediated antibody responses to NGVEGF prohibit SARS-CoV-2/ACE2 receptor binding

Mathematical models with pre-immunity could fully predict virus outbreak dynamics

Almazán et al., iScience 26, 108441
December 15, 2023
https://doi.org/10.1016/j.isci.2023.108441

iScience

CellPress
OPEN ACCESS

Article

Influenza-A mediated pre-existing immunity levels to SARS-CoV-2 could predict early COVID-19 outbreak dynamics

Nerea Martín Almazán,[1,2,3,15] Afsar Rahbar,[1,2,15,*] Marcus Carlsson,[4] Tove Hoffman,[5] Linda Kolstad,[5] Bengt Rönnberg,[5] Mattia Russel Pantalone,[1,2] Ilona Lewensohn Fuchs,[6,7] Anna Nauclér,[1] Mats Ohlin,[8] Mariusz Sacharczuk,[9,10] Piotr Religa,[1,2,10] Stefan Amér,[11] Christian Molnár,[11,12] Åke Lundkvist,[5] Andres Susrud,[13] Birger Sörensen,[13] and Cecilia Söderberg-Nauclér[1,2,14,16,17,*]

SUMMARY

Susceptibility to severe acute respiratory syndrome coronavirus 2 (SARS-CoV-2) infections is highly variable and could be mediated by a cross-protective pre-immunity. We identified 14 cross-reactive peptides between SARS-CoV-2 and influenza A H1N1, H3N2, and human herpesvirus (HHV)-6A/B with potential relevance. The H1N1 peptide NGVEGF was identical to a peptide in the most critical receptor binding motif in SARS-CoV-2 spike protein that interacts with the angiotensin converting enzyme 2 receptor. About 62%–73% of COVID-19-negative blood donors in Stockholm had antibodies to this peptide in the early pre-vaccination phase of the pandemic. Seasonal flu vaccination enhanced neutralizing capacity to SARS-CoV-2 and T cell immunity to this peptide. Mathematical modeling taking the estimated pre-immunity levels to flu into account could fully predict pre-Omicron SARS-CoV-2 outbreaks in Stockholm and India. This cross-immunity provides mechanistic explanations to the epidemiological observation that influenza vaccination protected people against early SARS-CoV-2 infections and implies that flu-mediated cross-protective immunity significantly dampened the first SARS-CoV-2 outbreaks.

INTRODUCTION

Severe acute respiratory syndrome coronavirus 2 (SARS-CoV-2) is considered a new virus to humans. Therefore, a major impact on people's health was expected when the virus began to spread around the globe in early 2020. Mathematical modeling predicted an infection rate of at least 70% within a few months, suggesting catastrophic scenarios of collapsed health care systems and high death tolls if strict nonpharmacological mitigation strategies were not implemented.[1] However, although many people have suffered and died, the catastrophic scenarios predicted did not come true. After the first wave, measured seroprevalence levels were less than 25% in a majority of hard-hit locations, and it was evident that SARS-CoV-2 infection affected people very differently. About 50% of infections caused by the original Wuhan strain were asymptomatic. Among people with symptomatic infections, 80% had mild symptoms, 20% developed severe disease and required hospital care, and 3%–5% were admitted to intensive care units.[2,3] People over 70 years of age and those with obesity, type II diabetes, or hypertension are at higher risk of severe COVID-19 disease,[4] and the impact on some patients, even young previously healthy people, can be unpredictable and disastrous.

[1]Department of Medicine, Unit for Microbial Pathogenesis, Karolinska Institutet, 17164 Solna, Stockholm, Sweden
[2]Department of Neurology, Karolinska University Hospital, 171 76 Solna Stockholm, Sweden
[3]Department of Laboratory Medicine, Division of Pathology, Karolinska Institutet, 141 86 Huddinge Stockholm, Sweden
[4]Centre for the Mathematical Sciences, Lund University, 223 62 Lund, Sweden
[5]Zoonosis Science Center (ZSC), Department of Medical Biochemistry and Microbiology (IMBIM), Uppsala University, 1477 Uppsala, Sweden
[6]Department of Labortory Medicine, Division of Clinical Microbiology, Karolinska Institutet, 141 86 Huddinge Stockholm, Sweden
[7]Department of Clinical Microbiology, Karolinska University Hospital, 141 86 Huddinge Stockholm, Sweden
[8]Department of Immunotechnology and SciLifeLab Human Antibody Therapeutics Infrastructure Unit, Lund University, 223 62 Lund, Sweden
[9]Faculty of Pharmacy with the Laboratory Medicine Division, Department of Pharmacodynamics, Medical University of Warsaw, Centre for Preclinical Research and Technology, Banacha 1B, 02-091 Warsaw, Poland
[10]Department of Experimental Genomics, Institute of Genetics and Animal Biotechnology, Polish Academy of Sciences, Postępu 36A, 05-552 Magdalenka, Poland
[11]Familjeläkarna Saltsjöbaden, 133 34 Saltsjöbaden, Sweden
[12]Department of Neurobiology, Care Sciences and Society, NVS, Karolinska Institutet, 171 77 Stockholm, Sweden
[13]Immunor AS, 0349 Oslo, Norway
[14]Institute of Biomedicine, Unit for Infection and Immunology, MediCity Research Laboratory, University of Turku, FI-20014 Turku, Finland
[15]These authors contributed equally
[16]Senior author
[17]Lead contact
*Correspondence: afsar.rahbar@ki.se (A.R.), cecilia.naucler@ki.se (C.S.-N.)
https://doi.org/10.1016/j.isci.2023.108441

In Sweden, we observed a decline of cases in larger cities from April 2020 even under less strict nonpharmacological interventions than in most other western countries. By May 2020, 19.1% of 2,149 staff members at Danderyd's Hospital in Stockholm tested positive for SARS-CoV-2 antibodies.[5] At several elder care homes in Stockholm and Uppsala in Sweden, about 23% of the personnel rapidly became antibody positive during the first wave.[6] In Sweden, a lockdown was never implemented, elementary and middle schools remained open, and until January 2021 face masks were not recommended, even in the care of vulnerable patients in hospitals. From mid-March 2020, high schools and universities were on distance learning in Sweden and people were expected to work from home and, if possible, avoid public transportation. Frequent hand washing, social distancing, and staying at home if feeling sick were the main recommendations from health authorities and the government. Nevertheless, cases declined already from April 2020, and, after the first wave, a seroprevalence of only 10% was reached in the general population in Stockholm by September 2020 (according to seroprevalence data from the Swedish Public Health Agency[7]).

We further observed that infection rates on cruise ships during the first wave also peaked at ~20%, even though many passengers were older than 70 years.[8,9] Also in New York, seroprevalence was 23.6% after the spring of 2020.[10] Furthermore, like observed for influenza virus and cold coronaviruses,[11] rarely more than 15%–20% of household members became infected with pre-Omicron SARS-CoV-2 strains by a family member with confirmed COVID-19.[12] We hypothesized that this pattern of declining viral spread and a suspected protection of about 75%–80% of the population from infection or severe COVID-19 disease before Omicron evolved is best explained by a pre-existing immunity. Such pre-immunity would also contribute to herd immunity thresholds. To test this hypothesis, we used mathematical models to study the effects of factors such as nonpharmacological interventions, age, interactive patterns, mobility, and pre-immunity on viral outbreaks. It proved impossible to match modeled and real data without incorporating a pre-existing immunity level of 50%–60%.[13,14]

If existing, a pre-immunity to SARS-CoV-2 is most likely mediated by previous infections. Indeed, 40%–60% of healthy blood donors, including those giving blood before SARS-CoV-2 existed, have T cells that respond to SARS-CoV-2 peptides *in vitro*.[15–20] T cells expanded to stimulation with SARS-CoV-2 peptides *in vitro*, particularly in samples from patients with abortive infections.[19] Such T cell pre-immunity was implied to be caused by common cold coronaviruses[20–24] and could contribute to herd immunity levels.[25–27] In support of this hypothesis, T cells cross-reactive with human coronaviruses and SARS-CoV-2 epitopes (spike, nucleocapsid, membrane, envelope, and ORF1; Open Reading Frame 1) were prominent in contacts who did not become PCR positive despite SARS-CoV-2 exposure.[20] Hence, in some people, T cells that are trained to recognize unrelated pathogen peptides may protect against COVID-19 through cross-protective immunity. However, as SARS-CoV-2 can be transmitted by aerosols,[28] antibody protection is expected to be required in addition to T cells to protect against infection with SARS-CoV-2 on a population level, as they can contribute to the first-line defense of an invading virus.

Neutralizing antibodies to SARS-CoV-2 have been found in pre-pandemic human antibody gene libraries.[29] One report suggested that 44% of children and 5.7% of adults have antibodies to common cold coronaviruses that can confer neutralizing activity against SARS-CoV-2.[23] However, although such cross-reactive antibodies potentially could have been raised by common cold coronaviruses,[22] and be boosted by SARS-CoV-2 infection, these were not considered protective.[30] Furthermore, this low level of pre-immunity in adults would not explain the slowdown of SARS-CoV-2 spread when about 20% of a population becomes infected. We therefore set out to identify the source of a pre-immunity that could explain the viral spread pattern and pathogenesis, by searching for potential cross-reactivities between SARS-CoV-2 and other pathogens.

RESULTS

Identification of potential cross-reactivities between SARS-CoV-2 and other pathogens

A BLAST search for cross-reactive protein sequences between SARS-CoV-2 and any other unrelated pathogen that could have mediated a cross-protective immunity identified SARS-CoV (2004) with 76% identity, MERS-CoV (2012) with 35.1% identity, and other pathogens such as non-human coronaviruses, human coronaviruses, and of interest two influenza A H1N1 strains, Nagasaki/07N005/2008 (NCBI: Accession: ADC45716.1) and Kyoto/07K520/2008 (NCBI/Genbank Accession: ADB89800.1), and influenza A H3N2 as well as human herpesvirus (HHV)-6A and HHV-6B (first BLAST search was performed in February 2020). At this time, SARS-CoV-2 sequences were not in the Uniprot database. Aiming to next search for cross-reactive epitopes between the SARS-CoV-2 spike protein and influenza A H1N1, influenza A H3N2, and HHV-6A proteins, we next used a method focusing on small 6-mer peptides that could represent possible small epitope targets for antibody binding[31] (gene bank reference NC_045512.2).

Interestingly, we identified a peptide in SARS-CoV-2, NGVEGF (Figure 1A), that is identical to a peptide in neuraminidase of the two influenza A H1N1 strains Nagasaki/07N005/2008 and Kyoto/07K520/2008. Remarkably, this peptide is present in the most critical part of the receptor binding motif of the spike protein (amino acids [aa] N481 to F486, Figure 1A) that interacts with the angiotensin converting enzyme 2 (ACE2) receptor (Figure 1B).[32] This peptide was present in an immunogeneic region of H1N1 neuraminidase (Figure 1C).[33] We also found another peptide, LKPFNR, present in influenza A H3N2, which is 83.3% similar to another epitope found in the receptor binding domain (RBD) of the SARS-CoV-2 spike protein, position 461–466 (LKPFER). An adjacent peptide, FERDIS in the RBD of spike (Figure 1D), was also similar to a peptide, FDRDIS, present in glycoprotein B (U39) of HHV-6A (in 43 of 43 proteins in gene bank) and HHV-6B (in 62 of 63 proteins present in databases). Another similar peptide, FERDIA, was found in a late glycoprotein (U22) in HHV-6A (in 33 of 33 proteins) and in HHV-6B (in 43 of 43 proteins).

NGVEGF, with its critical location in the spike protein for receptor interaction, was not found in any H1N1 strain sequenced before 2008 (Table 1). A variant, NGVKGF, was present in 99.3% of swine flu strains (n = 18,972) sequenced after 2008 and in 31.4% of strains (n = 1,467) sequenced before 2008 (Table 1). The NGVKGF peptide was also present in early SARS-CoV-2 variants from Brazil (gamma, P1), South Africa (beta, B.1.351, V 501Y.V2), and New York (iota, B.1.526), which carry the E484K mutation. The LKPFNR peptide was present in the PB1-F2

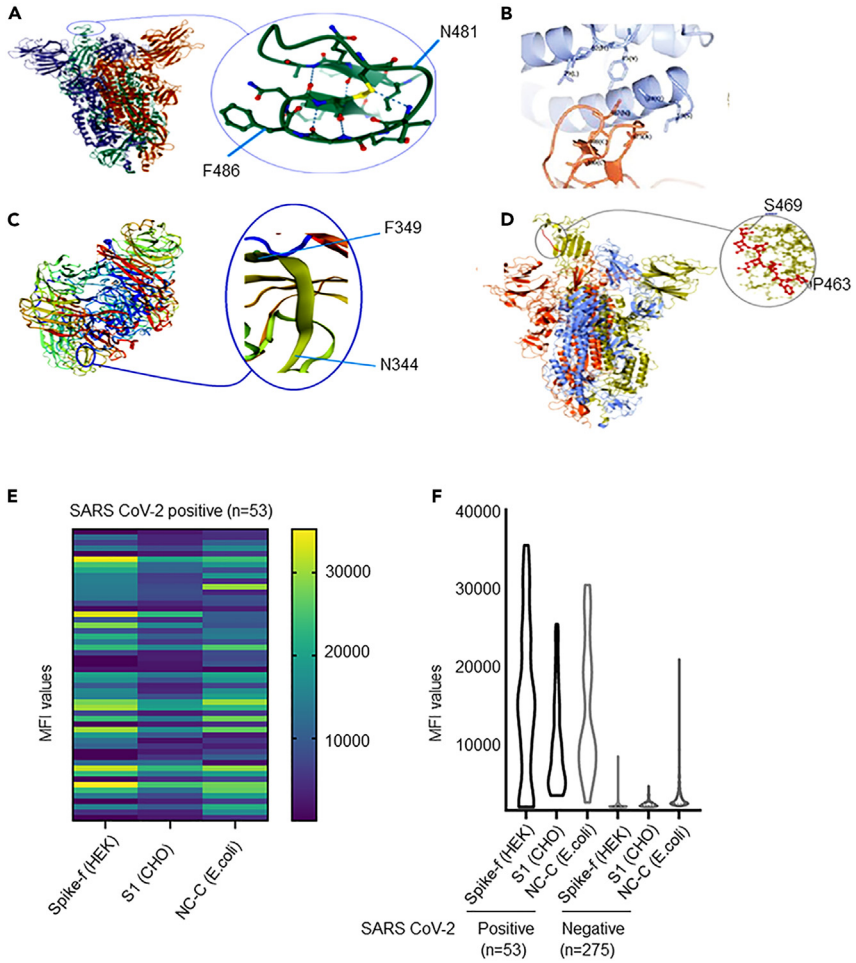

(figure continued on next page)

protein and was found only in 3 of 22,543 PB1 proteins in A/Florida/58/2019(H3N2) and A/South Australia/139/2015(H3N2) strains (gene bank: MN423441.1, CY253920.1, MN222088.1).

As flu strains containing NGVKGF are currently circulating around the globe and have been included in seasonal flu vaccines during the last decade, it is theoretically possible that antibodies to NGVEGF/NGVKGF, developed during influenza A H1N1 infections or after a seasonal flu vaccination, could have elicited an antibody response able to provide protection against pre-Omicron strains of SARS-CoV-2. Likewise, as about 70%–96%[34,35] of the population has been infected with HHV-6A and or HHV-6B, this virus could also have triggered peptide-specific antibody responses to the peptide LKPFERDIS and prevent SARS-CoV-2 to bind to the ACE2 receptor.

RBD-specific antibodies are present in COVID-19-negative individuals

Due to their presence in swine flu and HHV-6A/B, we hypothesized that the NGVEGF and/or LKPFERDIS peptides could have generated cross-protective immunity to SARS-CoV-2. To determine if peptide-specific antibodies to NGVEGF or LKPFERDIS are present in healthy unvaccinated COVID-19 negative individuals, we developed a diagnostic ELISA method to detect peptide-specific antibodies to NGVEGF or LKPFERDIS, respectively. We tested plasma/serum samples from 328 healthy persons collected during September to mid-October 2020 and analyzed the samples for the presence of immunoglobulin G (IgG)-specific antibodies to the SARS-CoV-2 spike protein and to the NGVEGF or LKPFERDIS peptides. Spike-specific antibodies were detected in 53 (16.2%) of 328 samples with a validated multiplex assay,[36] and we determined who among the donors were positive or negative for COVID-19 (Figures 1E and 1F). The prevalence of IgG positivity to NGVEGF was 73% among COVID-19-negative individuals using a threshold optical density (OD) value $\geq$ 0.2 and 62% at OD $\geq$ 0.3 (1:32 dilution, Figures 1G and 1H). The prevalence of IgG positivity to LKPFERDIS was also 73% among COVID-19-negative individuals, using a threshold

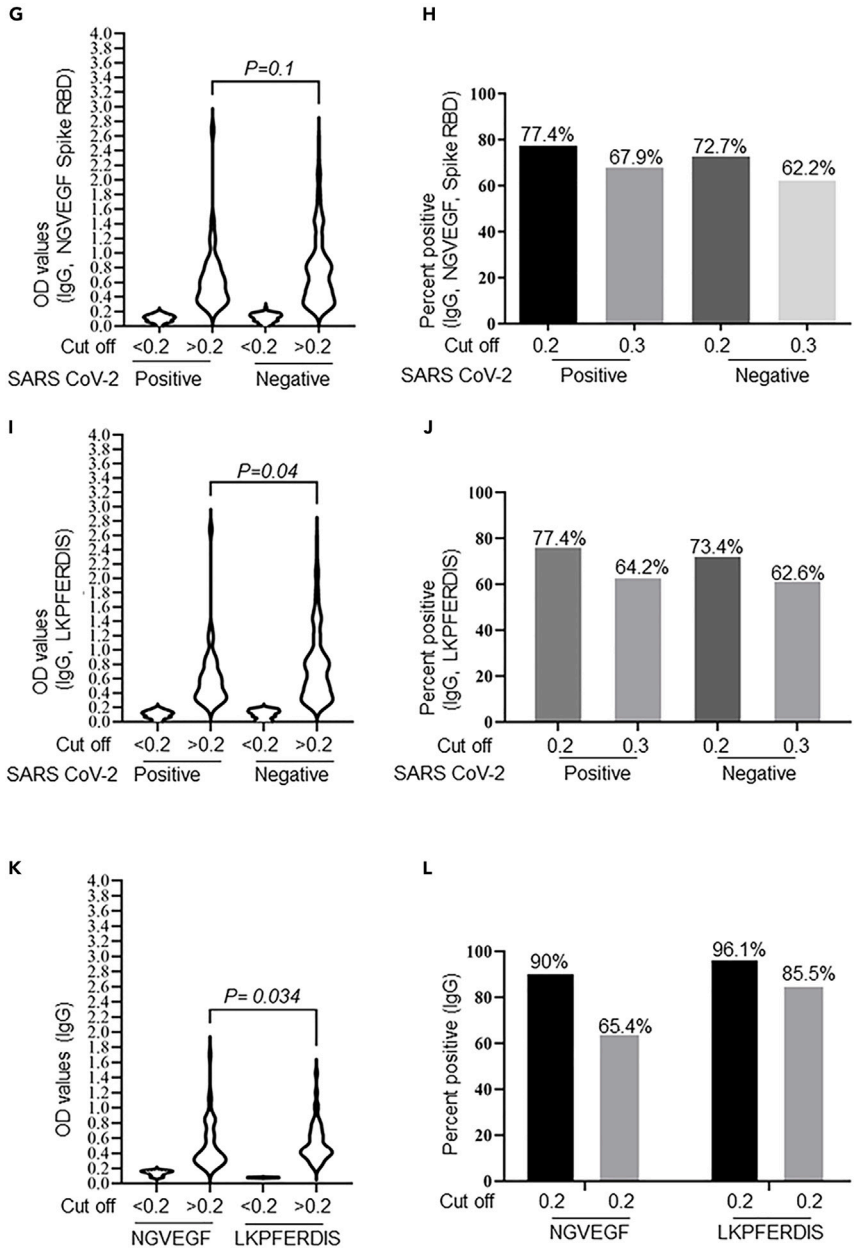

Figure 1. Influenza and HHV-6 peptides are identical to peptides in the RBD of the spike protein of SARS-CoV-2 and are recognized by antibodies in SARS-CoV-2-negative individuals

(A) Localization of the influenza A H1N1 NGVEGF peptide in the spike protein of SARS-CoV-2.

(B) NGVEGF is present in the critical domain of SARS-CoV-2 that interacts with the ACE2 receptor.

(C) NGVKGF is situated in an immunodominant region of the neuraminidase enzyme of influenza A H1N1.

(D) Localization of the HHV-6 peptide PFERDIS in the SARS-CoV-2 RBD.

(E and F) Fifty-three of 328 subjects had IgG antibodies (mean MFI >6 SD) against soluble pre-fusion stabilized trimeric spike glycoprotein (SPIKE-f (HEK)).

(G and H) NGVEGF-specific IgG antibody levels in COVID-19-positive and COVID-19-negative subjects, measured by ELISA.

(I and J) LKPFERDIS-specific IgG antibody levels in COVID-19-positive and COVID-19-negative subjects, measured by ELISA.

(K and L) NGVEGF- and LKPFERDIS-specific IgG antibody levels in serum samples from healthy donors in 2011, as measured by ELISA and prevalence of peptide-specific IgG antibody values (cutoff values are shown for OD $\geq$ 0.2 and >0.3) in healthy donors in 2011. (H and J) Prevalence of peptide-specific IgG antibody values (cutoff values are shown for OD > 0.2 and >0.3) in COVID-19-positive and COVID-19-negative subjects. (G and I) Unpaired t test was used to analyze the levels of IgG antibodies toward the same peptides in two different cohorts and (K) ratio paired t test was used to analyze the differences between the pairs for the levels of IgG antibodies toward different peptides in the same cohort. OD: Optical Density.

Table 1. Influenza H1N1 strains protein sequence for complete neuraminidase

H1N1-NA	NGVKGF	NGVEGF	NGIKGF	DGVKGF
Before 2008 (n = 1467)	461 (31.4%)	0 (0%)	1 (<0.01%)	990 (67.5%)
After 2008 (n = 18,972)	18,834 (99.3%)	2 (<0.01%)	12 (<0.01%)	107 (0.6%)

Data are from fludb.org.

OD value ≥ 0.2 and 63% at OD > 0.3 (1:32 dilution, Figures 1I and 1J). The prevalence of NGVEGF reactive antibodies trended higher at OD > 0.3 in COVID-19-positive individuals as compared to COVID-19-negative individuals (68% versus 62%), possibly indicating that the antibody levels to this peptide, but not to LKPFERDIS (64% versus 63%), were boosted by a SARS-CoV-2 infection. We next examined the prevalence of NGVEGF and LKPFERDIS reactive antibodies in pre-pandemic sera from a cohort of healthy blood donors collected in 2011. In this cohort, the levels of LKPFERDIS reactive IgG antibodies were higher than NGVEGF reactive antibodies ($p = 0.034$, Figure 1K). At an OD ≥ 0.2, 90% and 96% of sera and, at OD > 0.3, 65% and 86% of sera from 2011 contained NGVEGF and LKPFERDIS reactive IgG antibodies (Figures 1K and 1L), respectively. The antibody levels in sera from 2011 trended to be higher for both NGVEGF and LKPFERDIS compared to antibody levels in plasma collected in 2020.

Receptor binding motif-specific antibody levels to NGVEGF/NGVKGF trend to be higher in COVID-19-positive than in COVID-19-negative individuals

To test the variability of antibody levels to the NGVEGF and NGVKGF peptides, respectively, in COVID-19-positive and COVID-19-negative individuals, we next established a Luminex Multiplex bead array assay. Using this method, we confirmed a variable antibody reactivity to NGVEGF in human sera and observed a trend for higher reactivity to the most common flu peptide NGVKGF than to NGVEGF in sera from both COVID-19-positive (Figures 2A and 2B) and COVID-19-negative individuals (Figures 2C and 2D). Antibody levels to both NGVEGF and NGVKGF peptides trended to be higher in COVID-19-positive individuals than to COVID-19-negative individuals (Figure 2B) and were especially prominent in some COVID-19-negative subjects (Figure S1). This method also detected antibodies to LKPFERDIS in both COVID-19-positive (Figures 2E and 2F) and COVID-19-negative (Figures 2G and 2H) subjects, but the levels did not seem to be higher in COVID-19-positive subjects (Figures 3A and 3B).

Flu vaccination can enhance SARS-CoV-2 immunity

To examine if NGVEGF- or LKPFERDIS-specific antibody titers increase after flu and/or COVID-19 vaccination and if the neutralizing capacity of antibodies in plasma against SARS-CoV-2 was affected by vaccination, we collected plasma and blood cells from 20 individuals before and after flu and COVID-19 vaccination. Only 20 individuals were included in this evaluation, as when ethical permission was granted for the study in December of 2020, almost all flu vaccines had been administered in Sweden, and COVID-19 vaccinations were ready to start. Hence, only few subjects were identified eligible for the study.

For 19 subjects, we examined the NGVEGF-specific peptide antibody response before and after flu and COVID-19 vaccination and also tested their plasma in a surrogate virus neutralization test (sVNT) to assess if plasma antibodies could prohibit binding of the SARS-CoV-2 spike protein to the ACE2 receptor. Fourteen of 19 (73.7%) individuals responded to vaccination with enhanced neutralizing capacity in the sVNT test, which was further enhanced by COVID-19 vaccination (Figure 4A and Table 2). The antibody levels to the NGVEGF peptide increased in 6/7 individuals considered healthy ($p = 0.008$, Figure 4B), but not among the elderly people living in a nursing home (only 2/12 responded weakly with rising antibody levels [Figure 4C]). While neither the healthy subjects nor the elderly people in nursing home responded with higher antibody levels to LKPFERDIS after flu vaccination ($p = 0.34$ *and* $p = 0.15$, Figures 4D and 4E), both groups responded with higher antibody levels to LKPFERDIS after COVID-19 vaccination ($p = 0.016$ and 0.017, respectively, Figures 4D and 4E). In contrast, antibody levels to NGVEGF were lower after COVID-19 vaccination in most subjects (Figures 4B and 4C).

T cells expand in some individuals after flu vaccination

While antibodies may protect people from becoming infected, cytotoxic T cells are considered crucial to resolve life-threatening infections by killing virus-infected cells. In modeling analyses, we found that the flu peptide containing NGVEGF (analyzed as a 15 mer flu peptide) in theory can be presented to CD8 T cells by certain human leukocyte antigen (HLA) class I molecules (HLA-A*33:01, HLA-A*68:01, HLA-A*31:01, HLA-A*11:01); these are found in about 22.2% of Scandinavians (Table S2). In contrast, the LKPFERDIS containing 15 mer peptide had relatively low predicted MHC class I immunogenicity and had no predicted binders above similar threshold as for NGVEGF (Table S2). *In vitro*, we tested whether there was any difference in the ability of T cells to respond to the NGVEGF 15 mer peptide after flu vaccination. We observed significantly more interferon (IFN)-γ producing CD8 T cells that recognized the NGVEGF peptide after flu vaccination (mean increase from 0.1% to 6.9%, $p = 0.007$, Figure 4F). Eight of 20 (40%) individuals had a robust increase in the number of CD8 T cells reactive to the NGVEGF peptide (mean increase of 3.2%). Thus, as was predicted by the HLA modeling, the CD8-positive T cell response against the NGVEGF peptide increased prominently in some individuals after flu vaccination. IFN-γ-producing CD4 T cells reactive to the NGVEGF peptide also trended to be higher after flu vaccination (increased from 0.08% to 9.15% [one outlier] after vaccination, $p = 0.06$, Figure 4F).

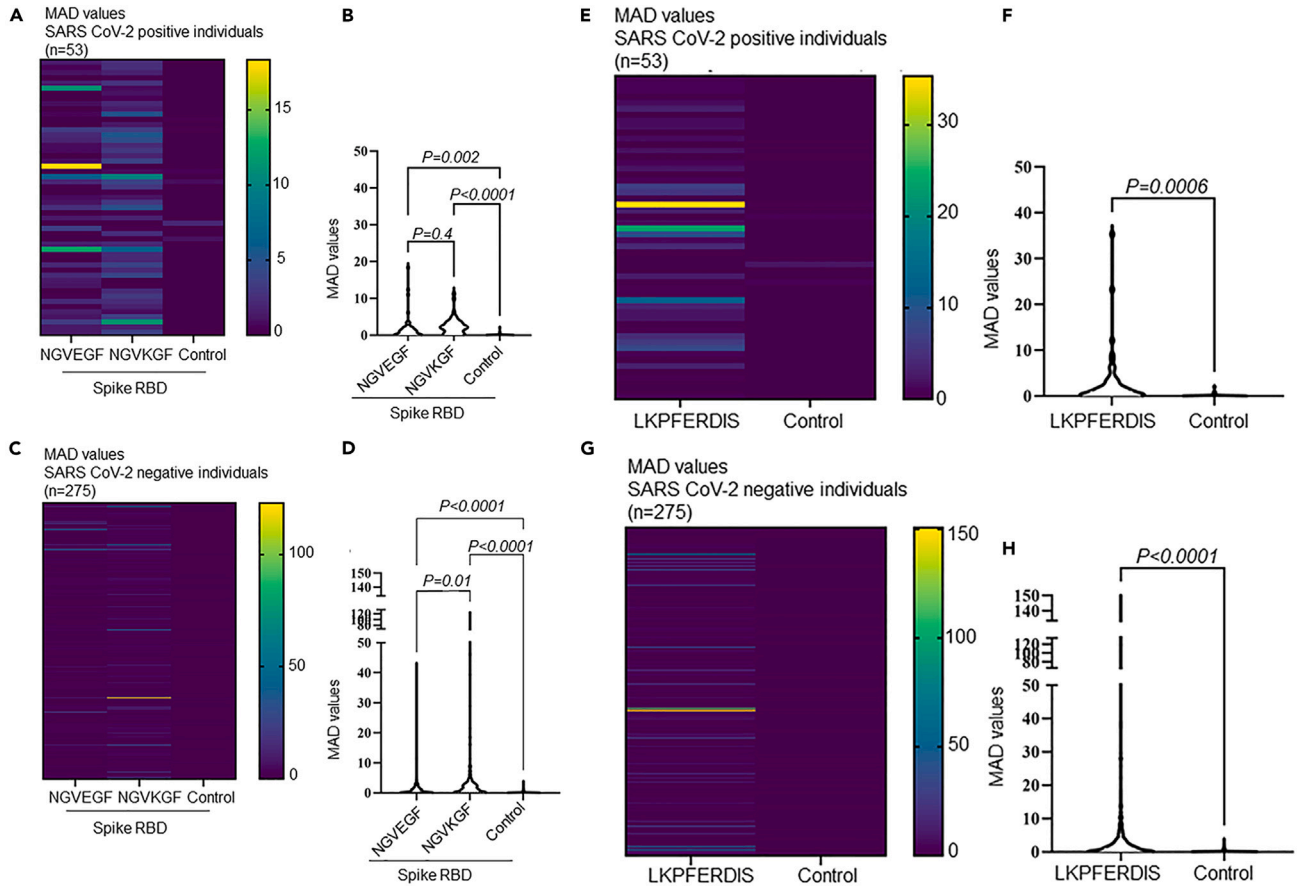

Figure 2. NGVEGF-, NGVKGF-, and LKPFERDIS-specific IgG antibodies are present in both COVID-19-positive and COVID-19-negative individuals

(A, C, E, G) Heatmap of MAD values for NGVEGF, NGVKGF, LKPFERDIS, and a control peptide (peptide 11) in COVID-19-positive (A) and COVID-19-negative (C) cohorts, and for LKPFERDIS in COVID-19-positive (E) and COVID-19-negative (G) cohorts. The IgG antibody levels (MAD values) to the NGVKGF peptide is higher than to the NGVEGF peptide in COVID-19-negative subjects (D), but not in COVID-19-positive subjects (B).

(F and H) The IgG antibody levels (MAD values) to the LKPFERDIS peptide was higher in COVID-19-positive subjects (F) and COVID-19-negative subjects (H) compared to control peptide.

(B and D) One-way ANOVA followed by Turkey's multiple comparison test was used for multiple comparisons to analyze median absolute deviations (MAD) for two different peptides (NGVEGF and NGVKGF) for COVID-19-positive and COVID-19-negative cohorts. (F and H) Paired t test was used to analyze the MAD values for one peptide (LKPFERDIS) for COVID-19-positive and COVID-19-negative cohorts compared to control peptide, respectively.

Flu-mediated protection to SARS-CoV-2 may vary in different populations

We next searched for additional T cell peptides that were shared between SARS-CoV-2 and influenza A H1N1. For this purpose, 15 mer epitopes from the influenza A H1N1 sequences were used to search for additional potential cross-reactivity between influenza A H1N1 and SARS-CoV-2 that could have mediated a protective T cell response to SARS-CoV-2. We identified 12 peptides that were similar between influenza A H1N1 and SARS-CoV-2 (including the NGVEGF peptide, Table S3). Modeling of HLA coverage implied that these 12 H1N1 peptides in theory could be presented by HLA types found in about 71% of people in Scandinavia (mainly by HLA-A*02:01 and HLA-A*01:01), but only in 40% of people worldwide (Table S2). These observations imply that the strength of SARS-CoV-2 protective immunity induced by influenza A strains may vary around the globe.

Mathematical modeling supports that the existence of a pre-existing immunity to SARS-CoV-2 dampened pandemic spread of the virus before Omicron emerged

To further understand whether a pre-existing flu-mediated cross-immunity to SARS-CoV-2 could have dampened the epidemic on a population level, we turned to mathematical models. We have earlier shown that the COVID-19 incidence data from Sweden cannot be explained by mathematical models unless we took some kind of pre-immunity into account in the model.[13,14] More precisely, we established that non-pharmaceutical interventions and voluntary updates in social patterns are highly unlikely to be the underlying reason for the relatively mild waves. The first wave affected about 10% of the population in Stockholm, despite the society was implementing neither lockdown-type

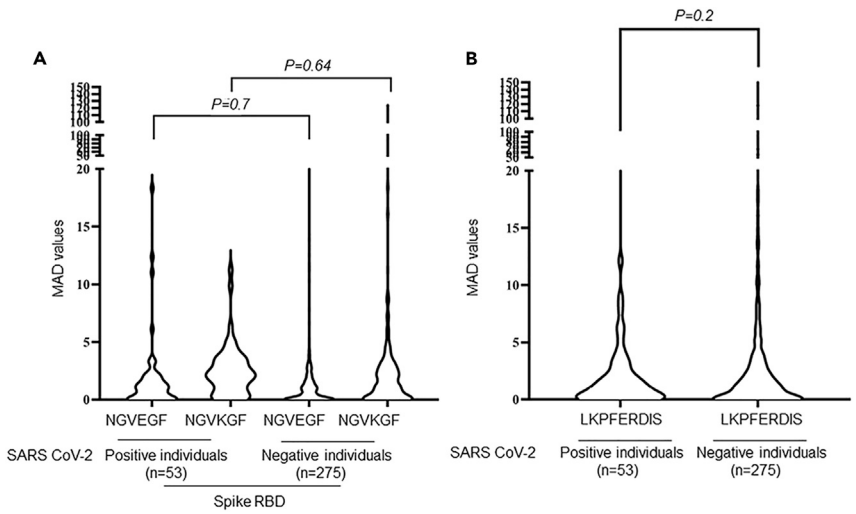

Figure 3. Levels of NGVEGF-, NGVKGF-, and LKPFERDIS-specific IgG antibodies in COVID-19-positive and COVID-19-negative individuals

(A) IgG antibody levels (MAD values) to NGVEGF and NGVKGF peptides in plasma from COVID-19-positive and COVID-19-negative individuals (A). IgG antibody levels (MAD values) to LKPFERDIS in plasma from COVID-19-positive and COVID-19-negative individuals (B). Unpaired t test was used to analyze MAD values in two different cohorts for different peptides.

measures nor face masks, and the second wave in late 2020 affected another 10%, according to seroprevalence data from the Swedish Public Health Agency.[7] We also established that invoking a pre-immunity in the range of 55%–65% into the model gave a surprisingly accurate match between model and measured data. This was the rationale for searching for the identity of a cross-protective pre-immunity, as we identified in the present study to possibly be mediated by flu.

The HLA modeling implied a potential variable efficiency of such protection in different populations due to different HLA types. We tested this hypothesis in our mathematical models. For this purpose, we implemented the SEIR model by Britton et al.,[37] taking interactive patterns between different age groups into account and variations in social activity (Age-Act SEIR, Figure 5A). This model was developed in an effort to demonstrate that social heterogeneity dampens model outcome, and hence this model is designed to produce mild waves. Despite this, we found that the model significantly overestimated the wave of infections when comparing modeled data to actual case data from Stockholm collected during the second wave (testing was not reliable during the first wave). For this analysis, data from the Swedish Public Health Agency allowed for separation of cases by the original versus the alpha strain that spread mainly during the third wave in Stockholm. Using either R_o value of 1.4 (Figure 5A) or 1.5 (Figure 5B), predictions could not match real case incidence during the second wave caused by the original strain only (readjusted to account for underreporting of cases, see the supplemental information for further details of preprocessing of the time series as well as modeling details).

We then ran the code including a pre-immunity level estimated from NGVEGF peptide-specific antibody levels of 73% (OD value > 0.2, R_o value of 1.5, Figure 5C) and 62% (OD > 0.3, Figure 5D), still taking the 10% seroprevalence from the first wave into account. Interestingly, we observed an almost perfect fit to measured data when we used the estimated contribution of the flu-mediated pre-immunity level of 62% (Figure 5D). Thus, when taking flu-mediated immunity and acquired immunity levels into account, it was fully possible to match modeled data to actual case data in Stockholm during the second wave (Figure 4D). It is hence possible that previous influenza A H1N1 infections/vaccinations could have protected a large part of the Swedish population against impact of SARS-CoV-2 outbreaks before Omicron emerged.

Our HLA-modeling data implied that the impact of SARS-CoV-2 may have varied around the globe, due to different HLA types in different populations. The modeled HLA class I-mediated protective T cell immunity levels for the Scandinavian population were estimated to be 71% according to expected HLA types in the population, which is also in the range of the prevalence levels for antibodies to the NGVEGF peptide (62%–73%, Figure 1H). The corresponding estimate for the world's population was 40%. We therefore hypothesized that a flu-mediated pre-immunity may have resulted in lower protection levels in other countries such as the hard-hit country India, than was observed for Stockholm. To test this hypothesis, we ran a more advanced version of the code on case data from India for the first and second wave. More precisely, we used the code developed previously,[13] which is an improvement of the code from Britton et al.,[37] which allows for incorporation of multiple strains with different R_o values and different pre-immunity levels. Upon fitting the model curve with actual case data from India (rescaled so that it corresponded to seroprevalence measurements, and accounting for underreporting and assuming an antibody half-life of 16 months after natural infection[38]), we found that using an estimated 30% pre-immunity against the original strain and a 15% pre-immunity for the delta variant (there was no alpha wave in India), the model fit the observed case data remarkably well (Figure 5E). These observations give further support to the hypothesis that a flu-mediated pre-immunity could have protected people against SARS-CoV-2 infections before Omicron emerged, and that this protection may have been different in different parts of the world.

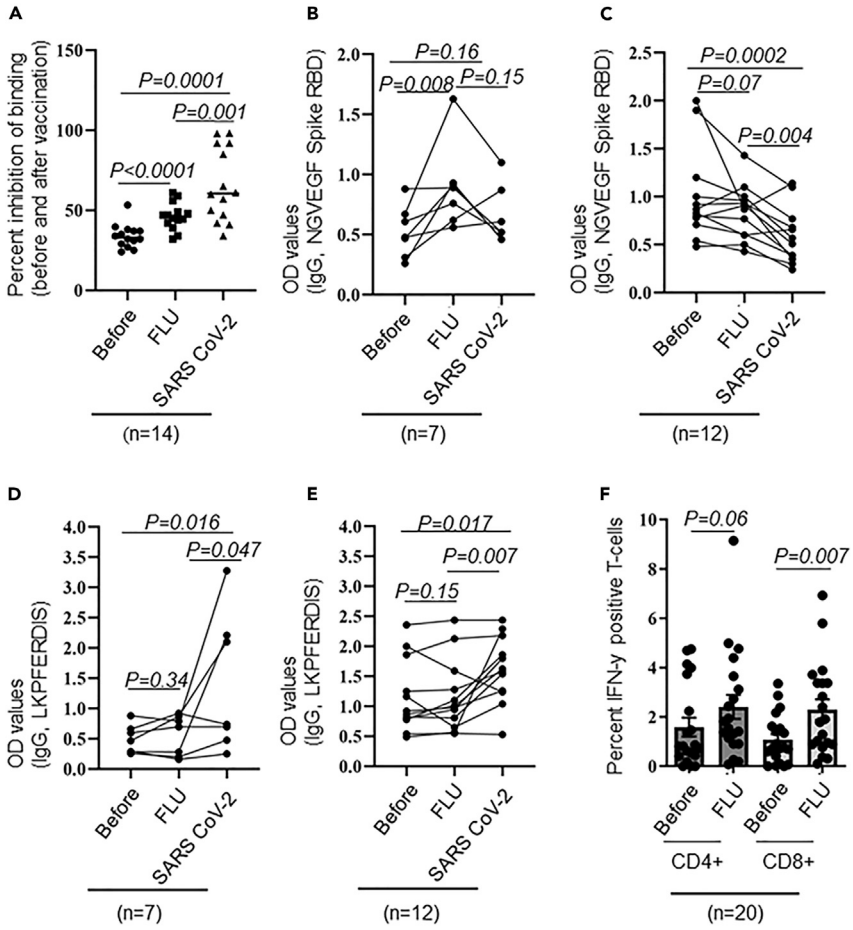

Figure 4. SARS-CoV-2-specific immunity increase in some individuals after flu vaccination

(A) Flu vaccination increased inhibition of binding of spike to the ACE2 receptor as assessed with a surrogate virus neutralization assay in 14 responding individuals.

(B) NGVEGF-specific IgG antibodies before and after flu and COVID vaccination in 7 healthy individuals and (C) in 12 elderly individuals living in an elderly home.

(D) LKPFERDIS-specific IgG antibodies before and after flu and COVID vaccination in 7 healthy individuals and (E) in 12 individuals living in an elderly home.

(F) Levels of IFN-γ producing CD4- and CD8-specific T cells stimulated with NGVEGF peptide before and after flu vaccination. Non parametric paired t test was used to analyze the same cohorts before and after vaccinations. Data are represented as mean ± SEM.

DISCUSSION

We discovered 12 peptides that are shared between influenza A H1N1 strains and SARS-CoV-2, one variant peptide that was shared with HHV-6A and HHV-6B, and one with influenza A H3N2. Two of these peptides NGVEGF (variant present in influenza A H1N1) and LKPFERDIS (variants present in H3N2 and HHV-6A/B) were interestingly localized to the RBD of the SARS-CoV-2 spike protein (Figures 1A and 1D). Remarkably, NGVEGF/NGVKGF peptides are present in neuraminidase of most influenza A H1N1 strains that have circulated around the globe during the last decades and were identical to the most important receptor binding motif of the SARS-CoV-2 spike protein that interacts with the ACE2 receptor. We provide evidence that 62%–73% of COVID-19-negative individuals had existing antibodies to the NGVEGF peptide, which could have mediated some protection against SARS-CoV-2 during the early phase of the pandemic when more pathogenic SARS-CoV-strains were circulating. The antibody levels to the NGVEGF peptide increased in healthy subjects but not in elderly people after flu vaccination. This peptide can also be presented to T cells, and the CD8-positive T cell response to the NGVEGF peptide also increased after flu vaccination in 73.7% of subjects ($p = 0.007$).

LKPFERDIS reactive antibodies were found in 63%–73% of COVID-negative individuals in plasma samples collected in 2020 and in 86.5%–96.1% of serum collected in 2011. Antibody levels to the LKPFERDIS peptide did not increase in any of the groups after flu vaccination but increased in both groups after COVID-19 vaccination ($p = 0.047$ and 0.007, respectively, Figures 4D and 4E). This was not the case for the antibody response to NGVEGF, which instead decreased after COVID-19 vaccination in the elderly cohort but was unaffected among those in the healthy group ($p = 0.004$ and $p = 0.15$, respectively, Figures 4B and 4C). The reason for this is unknown, but this implies different antibody responses to these two peptides after flu or COVID-19 vaccination, respectively. This LKPFERDIS peptide was not predicted to be a

Table 2. Detection of anti-SARS-CoV-2 antibodies before vaccination, after flu vaccination, and after COVID-19 vaccination using a COVID-19 suspension immunoassay (SIA) and a SARS-CoV-2 surrogate virus neutralization test (sVNT)

	Cohort				COVID-19 SIA (S1) Cutoff: 300 MFI Isotype: IgG	SARS-CoV-2 sVNT (S1) Cutoff: 36% Isotypes: All	IgG Targeting NGVEGF, Spike, RBD (OD)	IgG Targeting LKPFERDIS (OD)	IFN-γ positive $CD4^+$ T cells (%)	IFN-γ positive $CD8^+$ T cells (%)
Individual	Sampling	Previous flu infection/ Flu vaccination	Age (Year)	Sex (M/F)	MFI Interpretation (P/N)	Binding inhibition (%)				
1.	Before vacc	No/Yes (every year)	101	M	0	21	0.83	0,8257	0.55	0.07
1.	After flu vacc				0	23	0.60	0,80975	2.74	0.1
1.	After COVID-19 vacc				4490 P	79	0.66	1,54165	ND	ND
2.	Before vacc	No/not known	82	M	0	56	0.87	0,8659	1.37	1.62
2.	After flu vacc				0	32	1.1	1,008	1.54	1.29
2.	After COVID-19 vacc				2864 P	59	0.77	1,6262	ND	ND
3.	Before vacc	No/Yes (every year)	80	F	0	24	0.78	0.78	0.62	0.1
3.	After flu vacc				1	42	0.91	1.1	2.44	5.8
3.	After COVID-19 vacc				3617 P	65	0.51	1.86	ND	ND
4.	Before vacc	No/Yes (every year)	79	F	0	37	0.92	0.92	2.24	0.73
4.	After flu vacc				0	44	0.93	0.98	1.38	1.03
4.	After COVID-19 vacc				3037 P	57	0.68	1.26	ND	ND
5.	Before vacc	No/Yes (every year)	76	F	0	34	0.80	0.80	0.44	0.71
5.	After flu vacc				0	39	0.77	0.95	1.32	0.77
5.	After COVID-19 vacc				3347 P	61	0.39	1.8	ND	ND
6.	Before vacc	Yes (2019)/Yes (every year)	95	F	0	29	1.0	2,3598	0.17	2.38
6.	After flu vacc				0	34	0.96	2,43945	1.82	3.72
6.	After COVID-19 vacc				567 P	42	0.35	2,43945	ND	ND
7.	Before vacc	No/Yes (every year)	94	F	0	31	0.54	0.54	4.14	2.17
7.	After flu vacc				0	45	0.43	0.55	3.12	3.38
7.	After COVID-19 vacc				6139 P	85	0.3	0.53	ND	ND
8.	Before vacc	Not known/Not known	89	F	1363 P	52	0.71	1,16595	0.81	0.6
8.	After flu vacc				1066 P	49	0.61	0,65125	0.91	0.89
8.	After COVID-19 vacc				10,800 P	99	0.39	1,04	ND	ND
9.	Before vacc	No/yes	91	F	0	37	1.2	1.25	3.74	1.35
9.	After flu vacc				1	47	1.0	1.28	1.41	2.4
9.	After COVID-19 vacc				759 P	34	0.57	1.58	ND	ND
10.	Before vacc	Don't know/Yes	85	F	0	27	1.9	1.86	4.7	3.35

(*Continued on next page*)

Table 2. *Continued*

	Cohort				COVID-19 SIA (S1) Cutoff: 300 MFI Isotype: IgG	SARS-CoV-2 sVNT (S1) Cutoff: 36% Isotypes: All	IgG Targeting NGVEGF, Spike, RBD (OD)	IgG Targeting LKPFERDIS (OD)	IFN-γ positive $CD4^+$ T cells (%)	IFN-γ positive $CD8^+$ T cells (%)
10.	After flu vacc				4	32	1.43	2.13	4.99	3.38
10.	After COVID-19 vacc				1635 P	50	1.1	2.18	ND	ND
11.	Before vacc	Yes/Yes (every year)	66	M	0	32	0.48	0.49	4.75	1.53
11.	After flu vacc				0	47	0.5	0.57	1.94	0.37
11.	After COVID-19 vacc				2857 P	60	0.24	2.29	ND	ND
12.	Before vacc	No/Yes (every year)	85	M	0	32	2.0	2.0	1.47	0.76
12.	After flu vacc				0	48	0.87	1.59	0.08	0.31
12.	After COVID-19 vacc				23	41	1.14	1.24	ND	ND
13.	Before vacc	Yes (2018)/No	80	F	0	50	0.88	0.88	0.81	0
13.	After flu vacc				0	45	0.84	0.79	3.65	3.89
13.	After COVID-19 vacc				4517 P	84	0.53	3.28	ND	ND
14.	Before vacc	Yes (2018)/Yes (every year)	79	M	0	53	0.48	0.29	0	1.41
14.	After flu vacc				0	59	0.56	0.28	0.19	1.79
14.	After COVID-19 vacc				9850 P	98	0.61	2.21	ND	ND
15.	Before vacc	Yes (2016)/No	58	M	9	47	0.26	0.259	0	0
15.	After flu vacc				0	40	0.93	0.20	4.77	2.83
15.	After COVID-19 vacc				1762 P	59	0.46	0.48	ND	ND
16.	Before vacc	Yes/No	29	F	0	40	0.31	0.30	0.41	0.91
16.	After flu vacc				0	45	0.62	0.16	0.26	0.86
16.	After COVID-19 vacc				1430 P	47	0.87	0.25	ND	ND
17.	Before vacc	Yes (2015)/Yes (every year)	80	M	167	38	0.61	0.60	0.86	0.2
17.	After flu vacc				244	61	0.76	0.70	0.91	3.3
17.	After COVID-19 vacc				7598 P	98	0.52	0.70	ND	ND
18.	Before vacc	Yes (2015)/Yes (every year)	70	F	0	35	0.47	0.47	0.73	2.87
18.	After flu vacc				0	56	0.91	0.87	1.15	1.91
18.	After COVID-19 vacc				8595 P	92	0.47	2.1	ND	ND
19.	Before vacc	No/Yes (every year)	70	M	0	25	0.67	0.66	0	0.02
19.	After flu vacc				0	49	1.63	0.92	4.4	0.95
19.	After COVID-19 vacc				6611 P	92	1.1	0.74	ND	ND

Detection of antibodies targeting NGVEGF (in spike, RBD) and LKPFERDIS (in spike, RBD) peptides and percent IFN-γ positive $CD4^+$ and $CD8^+$ T cells after stimulation with NGVEGF (as 15-mer spike peptide) before and after vaccinations.

M; male, F; female, P; positive, MFI; mean fluorescence intensity, vacc; vaccination, S1; spike 1, OD; Optical Density.

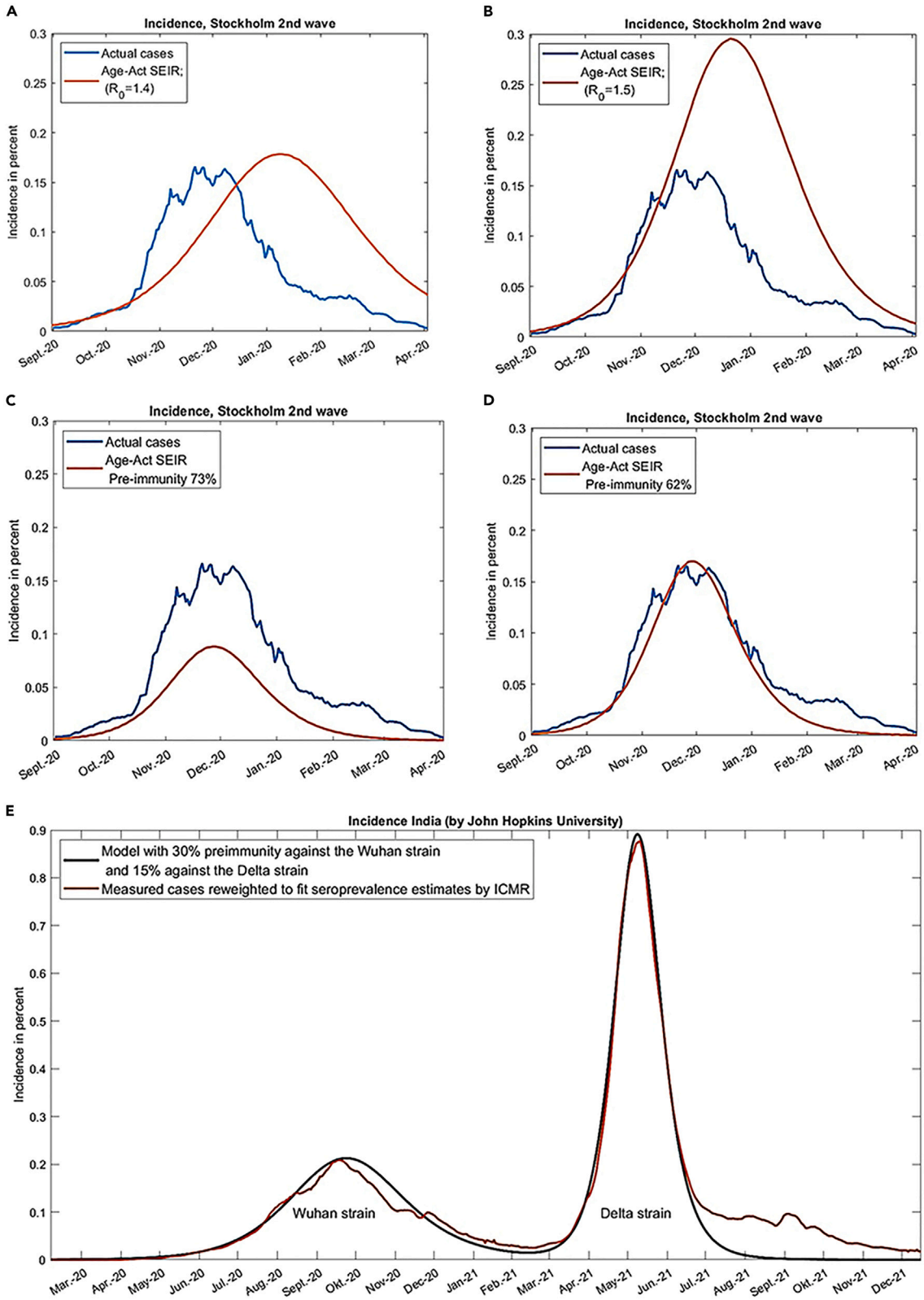
A
Incidence, Stockholm 2nd wave
Actual cases
Age-Act SEIR;
(R_0=1.4)
Incidence in percent
B
Incidence, Stockholm 2nd wave
Actual cases
Age-Act SEIR;
(R_0=1.5)
Incidence in percent
C
Incidence, Stockholm 2nd wave
Actual cases
Age-Act SEIR
Pre-immunity 73%
Incidence in percent
D
Incidence, Stockholm 2nd wave
Actual cases
Age-Act SEIR
Pre-immunity 62%
Incidence in percent
Sept.-20
Oct.-20
Nov.-20
Dec.-20
Jan.-20
Feb.-20
Mar.-20
Apr.-20
E
Incidence India (by John Hopkins University)
Model with 30% preimmunity against the Wuhan strain
and 15% against the Delta strain
Measured cases reweighted to fit seroprevalence estimates by ICMR
Incidence in percent
Wuhan strain
Delta strain
Mar.-20
Apr.-20
May-20
Jun.-20
Jul.-20
Aug.-20
Sept.-20
Okt.-20
Nov-20
Dec-20
Jan-21
Feb.-21
Mar.-21
Apr.-21
May-21
Jun.-21
Jul.-21
Aug.-21
Sept.-21
Okt.-21
Nov-21
Dec-21

Figure 5. Mathematical modeling considering estimated pre-existing immunity can predict COVID-19 outbreaks with high accuracy

Without taking pre-immunity into account, it was not possible to match the development of the second wave in Stockholm County using the heterogeneous Age-Activity stratified SEIR model developed by Britton et al.[37] The blue curves in panels A–C represent actual COVID-19 cases during the second wave in Stockholm. Attempts to fit actual cases in the absence of pre-immunity, using an R_0 value of 1.4 (A) or 1.5 (B) were unsuccessful. The model was tested with the estimated two pre-immunity levels identified in people in Stockholm for Influenza A H1N1: (C) OD value 0.2, 73% pre-immunity level (R_0 value of 1.5) and (D) for an OD value 0.3, 62% pre-immunity level (D). (E) The model could predict COVID-19 outbreaks with high accuracy using a pre-immunity level of 62% and an R_0 value of 1.5. The pandemic progression could also be accurately modeled for India, using an estimated pre-immunity of 30% against the original Wuhan strain and a 15% pre-immunity for the delta variant (estimated lower than in Stockholm due to a population with less beneficial HLA types to present flu peptides compared with people in Scandinavia). R_0 value of 1.5.

T cell peptide, wherefore not investigated further in the T cell assay. As the immune response to the NGVEGF peptide appears to be modulated by both flu and COVID-19 vaccination, this may have affected the consequences of COVID-19 infections in relation to timing of flu vaccinations in some people.

Antibody levels trended to be higher to both NGVEGF and LKPFERDIS peptides in sera collected in 2011 than in plasma collected in 2020. This was 3 years after swine flu emerged, and antibody levels to NGVEGF/NGVKGF peptides may therefore be higher in individuals who were recently infected or vaccinated against swine flu. Why antibody levels to LKPFERDIS were also higher is not known, as no epidemiological data exist on HHV-6A/B epidemics in the society.

Mathematical modeling using the estimated seroprevalence data of 62% for NGVEGF could accurately predict the outcome of case numbers in real life in Stockholm and hence gave further support to the hypothesis that a common flu-mediated pre-immunity have mediated a protection against SARS-CoV-2 infections. This discovery provides mechanistic explanations to the epidemiological observations that seasonal flu vaccination provided significant protection against COVID-19 infections, hospitalizations, intensive care unit (ICU) admission, and death[39–43], with estimated protection rates of 40%–80% that are in range of what was estimated in the present study (62%–73% for antibodies and 40%–71% for T cells). HLA modeling showed that flu/SARS-CoV-2 protective peptides can be presented by HLA types present in 71% of Scandinavians, but only in 40% of the world's population. Considering this, a flu-mediated protective immunity against SARS-CoV-2 may vary in different populations around the globe. Indeed, our mathematical modeling of SARS-CoV-2 outbreaks in Stockholm versus India showed this to be theoretically possible. In further support of the scenario that flu-mediated immunity has provided protection to SARS-CoV-2 infections, Pallikkuth et al. observed that 40% of COVID-negative individuals in Miami, Florida, exhibited a T cell response against SARS-CoV-2 peptides.[44] They observed that flu-specific T cell responses were strongly correlated with SARS-CoV-2-specific CD4 T cell responses, which supports the existence of a cross-reactive influenza-specific T cell immunity possibly providing immune protection to SARS-CoV-2 infections,[44] and this is in line with our predictions and estimations from collected data.

The identified cross-reactive pre-immunity is not expected to provide sterilizing immunity to SARS-CoV-2. Rather, we mainly consider that it acted as a brake on the epidemic viral spread, as a higher viral dose was likely needed to infect someone who had a substantial level of flu-mediated pre-immunity under given non-pharmacological interventions. More importantly, we consider the possibility that flu-mediated immunity may have protected many people from severe COVID-19 disease, perhaps especially if they had a recent influenza A infection or seasonal flu vaccination, which could have provided both antibody- and T cell-mediated immunity acting against SARS-CoV-2. This hypothesis is supported by the observed increase in NGVEGF-specific immunity to NGVEGF in some flu vaccinated individuals and by published epidemiological data suggesting that flu vaccinations provided protection against SARS-CoV-2.[44] The relevance of LKPFERDIS reactive antibodies is predicted to be low, as we found no increase of their levels after flu vaccination and there is no evidence of cross-reactive T cell peptides between HHV-6 and SARS-CoV-2.

Since many people have some NGVEGF/NGVKGF reactive antibodies, these new insights could affect the interpretation of the role of NGVEGF-specific antibodies in SARS-CoV-2-infected individuals, especially concerning their protective effects against variant viral strains containing the E484K, E484Q mutations or the E484A Omicron mutation.[44] One can then speculate over the following scenario; if this cross-protective immunity had not existed, is it possible that we could have experienced a very rapid spread of the original strain as was observed with Omicron,[12] which avoided both natural immunity, vaccination immunity, and influenza pre-immunity, and therefore had a more similar spread pattern as was expected by the early mathematical modeling? The original Omicron strain had 32 mutations, including critical mutations in the RBD (S477N, T478K, E484A, Q493R, G496S, Q498R, N501Y, and Y505H).[45] As this region is targeted by flu- and SARS-CoV-2-specific antibodies, these mutations were likely established to avoid both flu and SARS-CoV-2 immunity. The E484A Omicron mutation changes glutamic acid (E) to alanine (A481) in position 484 in the receptor binding motif of the spike protein that interacts with the ACE2 receptor. This mutation will make the core part (483V,484A) hydrophobic and limits its surface exposure and also changes the charge of this region and thereby limits the ability of antibodies to bind to the NGVEGF peptide in the spike protein. We therefore predicted that Omicron would overcome the flu-mediated pre-immunity, as well as the infection- or vaccination-mediated immunity that covers a larger part of the RBD (with 7 additional mutations). Previously,[13] we showed that it was possible to model the third wave quite well when including a pre-immunity of about 50%, suggesting that the flu-mediated immunity was effective also against the alpha strain, but then this immunity was lost to Omicron that rapidly infected a large proportion (40%–70%) of the population. As was expected from these predictions, Omicron was highly contagious and rapidly spread over the world, with high transmission rates also among vaccinated individuals and among those who already had been infected. Omicron infected up to 70% of the population in a given country within about 2–4 months.

Severity and mortality risk increases did not follow, most likely due to high vaccination coverage and a pre-existing T cell pre-immunity mediated by influenza A strains, common cold coronaviruses, and acquired immunity to early variants of the virus itself. Thus, if the spread

of the more pathogenic Wuhan strain causing more severe disease would have been as fast as Omicron spread among people lacking this cross-protective immunity, the pandemic could have been even more devastating than observed, and more in line with the predicted catastrophic scenarios early feared for by mathematical modeling. Therefore, this new knowledge of a potential flu-mediated protective immunity to early SARS-CoV-2 strains is important to take into account for future reliable mathematical modeling and political decisions in new pandemic situations, as future pandemics with a new infectious agent could be considerably worse if an underlying cross-protective immunity between common viruses and receptor binding interfering antibodies, as found here, are absent.

Limitations of the study

Our study is limited by the samples available for testing and the small group of individuals that could be included in the vaccination study. As most people have been exposed to flu in the past 10 years, no optimal negative samples were available for testing. It is not for certain that the antibodies that could bind to the NGVEGF peptide in *in vitro* assays could interact with the spike protein in SARS-CoV-2 in people. Furthermore, our modeling data also have limitations. First, levels of antibodies against NGVEGF, predicted T cell responses, and the neutralization assay have no threshold to estimate protection on an individual level and should be considered to be more relevant on a population level. Second, the mathematical model can only suggest a range of pre-immunity levels that are likely to be true in reality. Thus, both SEIR models and the method developed here are crude tools, and the results should be interpreted with caution. However, SIR (susceptible, infective, recovered) and SEIR models that did not include pre-immunity completely failed to predict the dynamics of SARS-CoV-2 spread. This is the main mathematical argument for the existence of a pre-existing immunity, the exact level of which is hard to estimate with certainty. On the other hand, the estimated pre-immunity levels from SEIR models and the completely different mathematical tool we devised for this study yielded remarkably consistent results, near the levels suggested by pre-immunity data presented here—supporting the existence of flu-mediated antibodies and T cells that cross-react with and protect against SARS-CoV-2 infection or from severe COVID-19 in a high proportion of Swedish people. This scenario would also explain why so many people in Sweden were not infected despite household exposure, had asymptomatic infections, or experienced mild disease while the society remained rather open.

We conclude that the possible high prevalence of flu-mediated cross-protective immunity to SARS-CoV-2 is relevant to consider in order to fully understand SARS-CoV-2 susceptibility, vaccine responses, protection against different virus variants, the natural course of COVID-19 in different individuals, and the impact of this virus and its mutants on our society.

STAR★METHODS

Detailed methods are provided in the online version of this paper and include the following:

- KEY RESOURCES TABLE
- RESOURCE AVAILABILITY
  - Lead contact
  - Materials availability
  - Data code availability
- EXPERIMENTAL MODEL AND STUDY PARTICIPANT DETAILS
  - Ethics statement
  - Identification of pre-immunity source
  - Samples
  - ELISA
- EXPERIMENTAL MODEL AND SUBJECT DETAILS
  - *In vivo* mouse model to test NGVEGF peptide antibody response
  - Serology with a suspension bead array
  - Identification of IFN-γ producing T cells by flow cytometry (FACS)
  - COVID-19 suspension immunoassay (SIA)
  - SARS-CoV-2 surrogate virus neutralization test (sVNT)
  - Mathematical modeling
- QUANTIFICATION AND STATISTICAL ANALYSIS

SUPPLEMENTAL INFORMATION

Supplemental information can be found online at https://doi.org/10.1016/j.isci.2023.108441.

ACKNOWLEDGMENTS

We thank the SciLifeLab Autoimmunity and Serology Profiling infrastructure unit for multiplex bead array serology and Cecilia Hellström, Peter Nilsson, and Sophia Hober for their valuable input to this study. We thank Benjamin Murrell and Daniel Scheward for performing an initial pseudo neutralization assay for the project and for their valuable input in discussions of our data. We thank Jonna Hermansson and Lisa

Lindberg for their help with sample collection at the elderly care home, and Koon Chu Yaiw for sample preparations. Finally, we thank Stephen Ordway for editorial help of early versions of this manuscript.

Funding: This research was partially funded by the Swedish Research Council (VR: 2019-01736, 2017-05807, 2018-02569), The European Union's Horizon 2020 Research Innovation Program under grant 874735 (VEO), The Knut and Alice Wallenberg Foundation, and the Science for Life Laboratory Uppsala (Projects: Nevermore Covid, SiCoV, and Molres), and Flagship InFLAMES through support from Academy of Finland.

AUTHOR CONTRIBUTIONS

Conceptualization: C.S.-N., M.C., A.S., B.S. Methodology: C.S.-N., A.R., B.R., P.R., A.S., S.A., Å.L., T.H., M.O., B.S., C.M., M.C., L.K., N.M.A. Software: M.C. Visualization: A.R., P.R., A.N., N.M.A. Validation: C.S.-N., A.R., B.R., P.R., Å.L., T.H., L.K., N.M.A. Formal analysis: C.S.-N., A.R., B.R., P.R., A.N., M.C. Investigation: A.R., B.R., P.R., I.L.F., M.R.P., S.A., Å.L., T.H., M.S., L.K., N.M.A. Resources: C.S.-N., P.R., I.L.F., M.R.P., S.A., Å.L., C.M. Data Curation: A.R., T.H., A.N., L.K., N.M.A. Funding acquisition: C.S.-N., Å.L. Project administration: C.S.-N., A.R., P.R. Supervision: C.S.-N., P.R., Å.L. Writing – original draft: C.S.-N. Writing – review & editing: C.S.-N., A.R., B.R., P.R., I.L.F., M.R.P., A.S., S.A., A.N., M.S., Å.L., T.H., M.O., B.S., C.M., M.C., L.K., N.M.A.

DECLARATION OF INTERESTS

B.S. and A.S. have submitted a patent application for a COVID-19 peptide vaccine.

Received: May 10, 2023
Revised: September 14, 2023
Accepted: November 9, 2023
Published: November 14, 2023

REFERENCES

1. Ferguson, N.M., Laydon, D., Nedjati-Gilani, G., Imai, N., Ainslie, K., Baguelin, M., Bhatia, S., Boonyasiri, A., Cucunubá, Z., Cuomo-Dannenburg, G., et al. (2020). Report 9: Impact of non-pharmaceutical interventions (NPIs) to reduce COVID-19 mortality and healthcare demand. Imperial College London *10*, 491–497.
2. Huang, C., Wang, Y., Li, X., Ren, L., Zhao, J., Hu, Y., Zhang, L., Fan, G., Xu, J., Gu, X., et al. (2020). Clinical features of patients infected with 2019 novel coronavirus in Wuhan, China. Lancet *395*, 497–506.
3. Zhou, F., Yu, T., Du, R., Fan, G., Liu, Y., Liu, Z., Xiang, J., Wang, Y., Song, B., Gu, X., et al. (2020). Clinical course and risk factors for mortality of adult inpatients with COVID-19 in Wuhan, China: a retrospective cohort study. Lancet *395*, 1054–1062.
4. O'Driscoll, M., Ribeiro Dos Santos, G., Wang, L., Cummings, D.A.T., Azman, A.S., Paireau, J., Fontanet, A., Cauchemez, S., and Salje, H. (2021). Age-specific mortality and immunity patterns of SARS-CoV-2. Nature *590*, 140–145.
5. Rudberg, A.S., Havervall, S., Månberg, A., Jernbom Falk, A., Aguilera, K., Ng, H., Gabrielsson, L., Salomonsson, A.C., Hanke, L., Murrell, B., et al. (2020). SARS-CoV-2 exposure, symptoms and seroprevalence in healthcare workers in Sweden. Nat. Commun. *11*, 5064.
6. Lindahl, J.F., Hoffman, T., Esmaeilzadeh, M., Olsen, B., Winter, R., Amer, S., Molnár, C., Svalberg, A., and Lundkvist, Å. (2020). High seroprevalence of SARS-CoV-2 in elderly care employees in Sweden. Infect. Ecol. Epidemiol. *10*, 1789036.
7. Agency, S.M.H. (2020). https://www.folkhalsomyndigheten.se/publikationer-och-material/publikationsarkiv/p/pavisning-av-antikroppar-mot-sars-cov-2-i-blodprov-fran-oppenvarden/.
8. Moriarty, L.F., Plucinski, M.M., Marston, B.J., Kurbatova, E.V., Knust, B., Murray, E.L., Pesik, N., Rose, D., Fitter, D., Kobayashi, M., et al. (2020). Public Health Responses to COVID-19 Outbreaks on Cruise Ships - Worldwide, February-March 2020. MMWR Morb. Mortal. Wkly. Rep. *69*, 347–352.
9. Expert Taskforce for the COVID-19 Cruise Ship Outbreak (2020). Epidemiology of COVID-19 Outbreak on Cruise Ship Quarantined at Yokohama, Japan, February 2020. Emerg. Infect. Dis. *26*, 2591–2597.
10. Pathela, P., Crawley, A., Weiss, D., Maldin, B., Cornell, J., Purdin, J., Schumacher, P.K., Marovich, S., Li, J., and Daskalakis, D.; NYC Serosurvey Team (2021). Seroprevalence of Severe Acute Respiratory Syndrome Coronavirus 2 Following the Largest Initial Epidemic Wave in the United States: Findings From New York City, 13 May to 21 July 2020. J. Infect. Dis. *224*, 196–206.
11. Casado, I., Martínez-Baz, I., Burgui, R., Irisarri, F., Arriazu, M., Elía, F., Navascués, A., Ezpeleta, C., Aldaz, P., and Castilla, J.; Primary Health Care Sentinel Network of Navarra (2014). Household transmission of influenza A(H1N1)pdm09 in the pandemic and post-pandemic seasons. PLoS One *9*, e108485.
12. Madewell, Z.J., Yang, Y., Longini, I.M., Jr., Halloran, M.E., and Dean, N.E. (2020). Household Transmission of SARS-CoV-2: A Systematic Review and Meta-analysis. JAMA Netw. Open *3*, e2031756.
13. Carlsson, M., and Soderberg-Naucler, C. (2022). COVID-19 Modeling Outcome versus Reality in Sweden. Viruses *14*, 1840.
14. Carlsson, M., Wittsten, J., and Söderberg-Nauclér, C. (2023). A note on variable susceptibility, the herd-immunity threshold and modeling of infectious diseases. PLoS One *18*, e0279454.
15. Grifoni, A., Weiskopf, D., Ramirez, S.I., Mateus, J., Dan, J.M., Moderbacher, C.R., Rawlings, S.A., Sutherland, A., Premkumar, L., Jadi, R.S., et al. (2020). Targets of T Cell Responses to SARS-CoV-2 Coronavirus in Humans with COVID-19 Disease and Unexposed Individuals. Cell *181*, 1489–1501.e15.
16. Braun, J., Loyal, L., Frentsch, M., Wendisch, D., Georg, P., Kurth, F., Hippenstiel, S., Dingeldey, M., Kruse, B., Fauchere, F., et al. (2020). SARS-CoV-2-reactive T cells in healthy donors and patients with COVID-19. Nature *587*, 270–274.
17. Le Bert, N., Tan, A.T., Kunasegaran, K., Tham, C.Y.L., Hafezi, M., Chia, A., Chng, M.H.Y., Lin, M., Tan, N., Linster, M., et al. (2020). SARS-CoV-2-specific T cell immunity in cases of COVID-19 and SARS, and uninfected controls. Nature *584*, 457–462.
18. Sekine, T., Perez-Potti, A., Rivera-Ballesteros, O., Strålin, K., Gorin, J.B., Olsson, A., Llewellyn-Lacey, S., Kamal, H., Bogdanovic, G., Muschiol, S., et al. (2020). Robust T Cell Immunity in Convalescent Individuals with Asymptomatic or Mild COVID-19. Cell *183*, 158–168.e14.
19. Swadling, L., Diniz, M.O., Schmidt, N.M., Amin, O.E., Chandran, A., Shaw, E., Pade, C., Gibbons, J.M., Le Bert, N., Tan, A.T., et al. (2022). Pre-existing polymerase-specific T cells expand in abortive seronegative SARS-CoV-2. Nature *601*, 110–117.
20. Kundu, R., Narean, J.S., Wang, L., Fenn, J., Pillay, T., Fernandez, N.D., Conibear, E., Koycheva, A., Davies, M., Tolosa-Wright, M., et al. (2022). Cross-reactive memory T cells associate with protection against SARS-CoV-2 infection in COVID-19 contacts. Nat. Commun. *13*, 80.
21. Ma, Z., Li, P., Ikram, A., and Pan, Q. (2020). Does Cross-neutralization of SARS-CoV-2 Only Relate to High Pathogenic

Coronaviruses? Trends Immunol. *41*, 851–853.
22. Jiang, S., and Du, L. (2020). Effect of Low-Pathogenic Human Coronavirus-Specific Antibodies on SARS-CoV-2. Trends Immunol. *41*, 853–854.
23. Ng, K.W., Faulkner, N., Cornish, G.H., Rosa, A., Harvey, R., Hussain, S., Ulferts, R., Earl, C., Wrobel, A.G., Benton, D.J., et al. (2020). Preexisting and de novo humoral immunity to SARS-CoV-2 in humans. Science *370*, 1339–1343.
24. Humbert, M., Olofsson, A., Wullimann, D., Niessl, J., Hodcroft, E.B., Cai, C., Gao, Y., Sohlberg, E., Dyrdak, R., Mikaeloff, F., et al. (2023). Functional SARS-CoV-2 cross-reactive CD4(+) T cells established in early childhood decline with age. Proc. Natl. Acad. Sci. USA *120*, e2220320120.
25. Doshi, P. (2020). Covid-19: Do many people have pre-existing immunity? BMJ *370*, m3563.
26. Sette, A., and Crotty, S. (2020). Pre-existing immunity to SARS-CoV-2: the knowns and unknowns. Nat. Rev. Immunol. *20*, 457–458.
27. Lipsitch, M., Grad, Y.H., Sette, A., and Crotty, S. (2020). Cross-reactive memory T cells and herd immunity to SARS-CoV-2. Nat. Rev. Immunol. *20*, 709–713.
28. Greenhalgh, T., Jimenez, J.L., Prather, K.A., Tufekci, Z., Fisman, D., and Schooley, R. (2021). Ten scientific reasons in support of airborne transmission of SARS-CoV-2. Lancet *397*, 1603–1605.
29. Bertoglio, F., Meier, D., Langreder, N., Steinke, S., Rand, U., Simonelli, L., Heine, P.A., Ballmann, R., Schneider, K.T., Roth, K.D.R., et al. (2021). SARS-CoV-2 neutralizing human recombinant antibodies selected from pre-pandemic healthy donors binding at RBD-ACE2 interface. Nat. Commun. *12*, 1577.
30. Anderson, E.M., Goodwin, E.C., Verma, A., Arevalo, C.P., Bolton, M.J., Weirick, M.E., Gouma, S., McAllister, C.M., Christensen, S.R., Weaver, J., et al. (2021). Seasonal human coronavirus antibodies are boosted upon SARS-CoV-2 infection but not associated with protection. Cell *184*, 1858–1864.e10.
31. Chen, C.W., and Chang, C.Y. (2017). Peptide Scanning-assisted Identification of a Monoclonal Antibody-recognized Linear B-cell Epitope. J. Vis. Exp. 55417.
32. Yang, J., Petitjean, S.J.L., Koehler, M., Zhang, Q., Dumitru, A.C., Chen, W., Derclaye, S., Vincent, S.P., Soumillion, P., and Alsteens, D. (2020). Molecular interaction and inhibition of SARS-CoV-2 binding to the ACE2 receptor. Nat. Commun. *11*, 4541.
33. Liu, W.C., Lin, C.Y., Tsou, Y.T., Jan, J.T., and Wu, S.C. (2015). Cross-Reactive Neuraminidase-Inhibiting Antibodies Elicited by Immunization with Recombinant Neuraminidase Proteins of H5N1 and Pandemic H1N1 Influenza A Viruses. J. Virol. *89*, 7224–7234.
34. Okuno, T., Takahashi, K., Balachandra, K., Shiraki, K., Yamanishi, K., Takahashi, M., and Baba, K. (1989). Seroepidemiology of human herpesvirus 6 infection in normal children and adults. J. Clin. Microbiol. *27*, 651–653.
35. Ihira, M., Yoshikawa, T., Ishii, J., Nomura, M., Hishida, H., Ohashi, M., Enomoto, Y., Suga, S., Iida, K., Saito, Y., et al. (2002). Serological examination of human herpesvirus 6 and 7 in patients with coronary artery disease. J. Med. Virol. *67*, 534–537.
36. Hober, S., Hellström, C., Olofsson, J., Andersson, E., Bergström, S., Jernbom Falk, A., Bayati, S., Mravinacova, S., Sjöberg, R., Yousef, J., et al. (2021). Systematic evaluation of SARS-CoV-2 antigens enables a highly specific and sensitive multiplex serological COVID-19 assay. Clin. Transl. Immunology *10*, e1312.
37. Britton, T., Ball, F., and Trapman, P. (2020). A mathematical model reveals the influence of population heterogeneity on herd immunity to SARS-CoV-2. Science *369*, 846–849.
38. Townsend, J.P., Hassler, H.B., Wang, Z., Miura, S., Singh, J., Kumar, S., Ruddle, N.H., Galvani, A.P., and Dornburg, A. (2021). The durability of immunity against reinfection by SARS-CoV-2: a comparative evolutionary study. Lancet. Microbe *2*, e666–e675.
39. Stowe, J., Tessier, E., Zhao, H., Guy, R., Muller-Pebody, B., Zambon, M., Andrews, N., Ramsay, M., and Lopez Bernal, J. (2021). Interactions between SARS-CoV-2 and influenza, and the impact of coinfection on disease severity: a test-negative design. Int. J. Epidemiol. *50*, 1124–1133.
40. Marín-Hernández, D., Schwartz, R.E., and Nixon, D.F. (2021). Epidemiological evidence for association between higher influenza vaccine uptake in the elderly and lower COVID-19 deaths in Italy. J. Med. Virol. *93*, 64–65.
41. Fink, G., Orlova-Fink, N., Schindler, T., Grisi, S., Ferrer, A.P.S., Daubenberger, C., and Brentani, A. (2020). Inactivated trivalent influenza vaccination is associated with lower mortality among patients with COVID-19 in Brazil. BMJ Evid. Based. Med. *26*, 192–193.
42. Conlon, A., Ashur, C., Washer, L., Eagle, K.A., and Hofmann Bowman, M.A. (2021). Impact of the influenza vaccine on COVID-19 infection rates and severity. Am. J. Infect. Control *49*, 694–700.
43. Debisarun, P.A., Gössling, K.L., Bulut, O., Kilic, G., Zoodsma, M., Liu, Z., Oldenburg, M., Rüchel, N., Zhang, B., Xu, C.J., et al. (2021). Induction of trained immunity by influenza vaccination - impact on COVID-19. PLoS Pathog. *17*, e1009928.
44. Pallikkuth, S., Williams, E., Pahwa, R., Hoffer, M., and Pahwa, S. (2021). Association of Flu specific and SARS-CoV-2 specific CD4 T cell responses in SARS-CoV-2 infected asymptomatic heath care workers. Vaccine *39*, 6019–6024.
45. Dejnirattisai, W., Huo, J., Zhou, D., Zahradník, J., Supasa, P., Liu, C., Duyvesteyn, H.M.E., Ginn, H.M., Mentzer, A.J., Tuekprakhon, A., et al. (2022). SARS-CoV-2 Omicron-B.1.1.529 leads to widespread escape from neutralizing antibody responses. Cell *185*, 467–484.e15.
46. Zhang, Y., Aevermann, B.D., Anderson, T.K., Burke, D.F., Dauphin, G., Gu, Z., He, S., Kumar, S., Larsen, C.N., Lee, A.J., et al. (2017). Influenza Research Database: An integrated bioinformatics resource for influenza virus research. Nucleic Acids Res. *45*, D466–D474.
47. Reynisson, B., Alvarez, B., Paul, S., Peters, B., and Nielsen, M. (2020). NetMHCpan-4.1 and NetMHCIIpan-4.0: improved predictions of MHC antigen presentation by concurrent motif deconvolution and integration of MS MHC eluted ligand data. Nucleic Acids Res. *48*, W449–W454.
48. Ayoglu, B., Mitsios, N., Kockum, I., Khademi, M., Zandian, A., Sjöberg, R., Forsström, B., Bredenberg, J., Lima Bomfim, I., Holmgren, E., et al. (2016). Anoctamin 2 identified as an autoimmune target in multiple sclerosis. Proc. Natl. Acad. Sci. USA *113*, 2188–2193.
49. Team, and and, R.C.R. (2019). A Language and Environment for Stastistical Computing (R Foundation for Stastistical Computing). https://www.R-project.org/.
50. Team, and Studio, R.R. (2018). Integrated Development for R (RStudio, Inc.). http://www.rstudio.com/.
51. Rahbar, A., Peredo, I., Solberg, N.W., Taher, C., Dzabic, M., Xu, X., Skarman, P., Fornara, O., Tammik, C., Yaiw, K., et al. (2015). Discordant humoral and cellular immune responses to (CMV) in glioblastoma patients whose tumors are positive for CMV. OncoImmunology *4*, e982391.
52. Hoffman, T., Kolstad, L., Lindahl, J.F., Albinsson, B., Bergqvist, A., Ronnberg, B., and Lundkvist, A. (2021). Diagnostic Potential of a Luminex-Based Coronavirus Disease 2019 Suspension Immunoassay (COVID-19 SIA) for the Detection of Antibodies against SARS-CoV-2. Viruses *13*, 993.

STAR★METHODS

KEY RESOURCES TABLE

REAGENT or RESOURCE	SOURCE	IDENTIFIER
Antibodies		
Anti-human IgG conjugated to Alkaline phosphatase-	Merck	Ca# AP113; RRID:AB_92435
Anti-human IgG conjugated R-phycoerthrin	Invitrogen	Ca# H10104; RRID:AB_465926
Anti-human IgG conjugated R-phycoerthrin	eBioscience	Ca# 12-4998-82; RRID:AB_465926
Anti-human CD4 eFlour	eBioscience	Ca# 48-0048-41; RRID:AB_2016607
Anti-human CD8 PE	eBioscience	Ca# 555635; RRID:ab-395997
Anti-interferon (IFN)-γ, FITC	BD BioSciences	Ca# 561057; RRID:AB_10562566
Anti-human IgG2b kappa, eFlour	eBioscience	Ca# 48-4732-80; RRID:AB_1272023
Anti-human IgG1 kappa, phycoerythrin	BD BioSciences	Ca# 555751; RRID:AB_398613
Anti-human IgG1, FITC	BD BioSciences	Ca# 554679; RRID:AB_395505
Biological samples		
Blood samples	Karolinska university Hospital (see ethics statement)	
Blood samples	Volunteers gave written informed consent for the study (see ethics statement)	
Blood samples	Elderly care home, Älvsjö, Stockholm (see ethics statement)	
Chemicals, peptides, and recombinant proteins		
Streptavidin	Sigma	Ca# SA101
Bovine serum albumin	Sigma	Ca# 9418
Tween-20	Amresco	Ca# 0777
Alkaline phosphatase substrate	Sigma	Ca# 7998
NaOH	Substrate at Karolinska University Hospital	
Neutravidin	Thermo Scientific	Neutravidin 31000
Paraformaldehyd	Alfa Aesar	Ca# 43368
Lymphoprep	Stem Cell Technologies	Ca# 7801
Brefelin A	Sigma	Ca# B6542
Phosphate buffered saline	Gibco	Ca# 14200067
Staphylococcal enterotoxin B domain	Sigma	Ca# S4881
PBS (phosphate buffered saline)	Gibco	Ca# 14200067
Propidium Iodide	Thermofisher	Ca# BMS500PI
sulfo-N-hydroxysulfosuccinimide (sulfo-NHS)	Thermofisher	Ca# 24525
Biotinylated protein G	Pierce Biotechnology, ThermoFisher Scientific	Ca# 29988
Streptavidin–phycoerythrin (SA-PE)	Invitrogen, ThermoFisher Scientific	Ca# S866
Biotinylated human angiotensin converting enzyme 2 (hACE2)	Sino Biological	Ca# 10108-H02H-B,
Tris	Sigma Aldrich	Ca# GE17-1321-01

(*Continued on next page*)

Continued

REAGENT or RESOURCE	SOURCE	IDENTIFIER
Color-coded magnetic microspheres	MagPlex, Luminex Corp.	-
FlexMap3D	Luminex Corp.	FLEXMAP-3D-RUO
Cytofix/Cytoperm	Life technologies	Ca# GAS004
1-ethyl-3-[3 dimethylaminopropyl]carbodiimide hydrochloride	Sigma Aldrich, Merck	Ca# 25952-53-8
Experimental models: Organisms/strains		
Mice (Swiss-Webster female mice aged 6–8 weeks)	Jackson Laboratories	
Software and algorithms		
Prism 9	GraphPad	https://www.graphpad.com/

RESOURCE AVAILABILITY

Lead contact

The datasets generated in the current study are available upon reasonable request by the lead contact, Cecilia Söderberg-Nauclér (cecilia.naucler@ki.se)

Materials availability

This study did not generate new unique reagents. Further information and requests for resources and reagents should be directed to and will be fulfilled by the lead contact.

Data code availability

All the necessary codes to reproduce the Figures 5A–5E can be downloaded at https://github.com/Marcus-Carlsson/Covid-modeling. Any additional information required to reanalyze the data reported in this paper is available from the lead contact upon request.

EXPERIMENTAL MODEL AND STUDY PARTICIPANT DETAILS

Ethics statement

The study was approved by the Ethics Committee at Karolinska Institutet, Stockholm, Sweden (Dnr 2020-06333: all vaccinated subjects gave written informed consent; blood donors from blood bank were anonymous; Dnr 2020-07232, Dnr 01-420). The study protocol for animal study was approved by II Local Ethics Committee for Animal Experiments in Warsaw (Dnr: 16.07.2021).

Identification of pre-immunity source

Initially an open blast was performed in February 2020 using uniprot.org\blast default settings against the whole SARS-CoV-2 Spike protein reference strain and any other unrelated pathogen identified SARS-CoV (2004) with 76% identity, MERS-CoV (2012) with 35.1% identity and other pathogens such as non-human coronaviruses, human coronaviruses and of interest Human Herpesvirus 6A/B, two Influenza A H3N2 strains; A/South Australia/139/2015 and A/Florida/58/2019 and two Influenza A H1N1 strains; Nagasaki/07N005/2008 and Kyoto/07K520/2008 (see results). Local BLAST analyses were next done with R (v3.5.3), RStudio (v1.1.463), and BLAST+ (v2.2.30+) to search for cross-reactive sequences between SARS-CoV-2 Human Herpesvirus 6A/B and Influenza. The database used was retrieved from Influenza Research Database (IRD) on September 8, 2020, with human as host for Influenza A and GenBank for Human Herpesvirus 6A/B. Blast was performed with the threshold (E-value) 1000, substitution matrix used was PAM-30, and the according gap cost and identified a hit to the SARS-CoV-2 spike protein. We analyzed the SARS-CoV-2 spike protein reference strain (YP_009724390) by using a rolling window of 6 amino acids (6-mers), which is the size of an antibody epitope and identified a hit to Influenza A H1N1 strains. 6-mers were blasted against the local influenza database with BLAST+ and the blastp routine in R. Subsequent data was obtained from the NIAID Influenza Research Database (IRD)[46] through the web site at http://www.fludb.org, and with links to relevant website pages in the body of the paper. The 6-mers were then blasted against the local influenza database and local Human Herpesvirus 6A/B U22 & U39 with BLAST+ and the blastp routine in R.

The 6 mer epitopes with similarity between SARS-CoV-2 and Influenza were then extended with 9 amino acids to 15mer epitopes from the Influenza A H1N1 sequences to search for potential cross reactivity between Influenza A H1N1 and SARS-CoV-2 that could mediate a potential protective T cell response. These 15mer epitopes were then further analyzed for potential ability to bind to different HLA class I molecules using the IEDB MHC I binding prediction tool. We identified 12 peptides similar between Influenza A H1N1 and SARS-CoV-2 that could theoretically bind HLA class I molecules, and potentially serve as T cell peptides. All positive binders with corresponding HLA alleles for binders predicted to be of <1% percentile rank were selected and we then modeled HLA coverage and potential T cell response among Scandinavians or the world's population for the 12 identified peptides. We used HLA allele frequency maps (pypop.org)[47] to calculate the global and Scandinavian HLA coverage for potential ability to respond to identified peptides. In contrast, the LKPFERDIS had relatively low predicted

MHC class I immunogenicity and had no predicted binders above similar threshold as used for NGVEGF (Table S2). The MHCI binding predictions were made on 5/30/2021 with the IEDB analysis resource NetMHCpan (v4.1) tool.[48]

Basic demographic characteristic of the study cohorts

Cohorts	Mean age (Year) (intervals)	Gender Female / Male (%)
Healthy donors from 2020 (n = 328)[a]	46.1[a] (18–83)	164 (50) / 164 (50)
Healthy donors from 2011 (n = 52)	39.5 (17–66)	26 (50) / 26 (50)
Flu and SARS-CoV-2 vaccinated (n = 19) (Seven healthy individuals had mean age of 66.6 years, twelve elderly individuals had mean age of 85.3 years)	78.4 (29–101)	11 (57.9)/ 8 (42.1)
Tested with SARS-CoV-2 surrogate virus neutralization test (sVNT) (n = 19)	78.4 (29–101)	11 (57.9) / 8 (42.1)
Analyzed for CD4 and CD8 T cells activity before and after flu vaccination (n = 20)	76.9 (29–101)	12(60) / 8 (40)

[a]Estimated gender and age data among whole cohort from 38,525 healthy anonymous blood donors from year 2020 in Stockholm at the blood bank in our hospital.

Samples

We collected plasma from 297 blood donors (September to first week in October 2020), and from 31 healthy individuals, all collected before Covid vaccines were introduced (during week 52 of 2020, mean age 46.1 years with intervals between 18-83 years, equal numbers of males and females, Figure 3 and above table) in Sweden. The blood donors were anonymous to the study team having donated blood to the blood bank at Karolinska University Hospital. Volunteers gave written informed consent for the study (see ethics statement). Blood samples (plasma and peripheral blood mononuclear cells (PBMCs) were also collected from 13 individuals at an elderly care facility (58-101 years old who all gave written informed consent for the study) in week 51 of 2020 before and at 4 weeks after FLU vaccination (VaxigripTetra Quadrivalent Flu vaccine (Sanofi Pasteur). Thereafter they received a Covid vaccination (after the sample was drawn), and an additional sample was drawn at 4 months after the COVID-19 vaccination during which time the subjects had received one booster dose. A similar sample series was collected from 7 healthy individuals aged 29-79 years old (all gave written informed consent for the study). We also analyzed 52 plasma samples from a cohort of healthy blood donors collected in 2011 after the Swine flu pandemic. These were also anonymous to the study team (mean age was 39.5 years with intervals between 17- 66 years, equal numbers of male and female).

Mouse sera were collected before, at 2 weeks post FLU vaccination (VaxigripTetra Quadrivalent Flu vaccine) and then at 4 weeks after combined FLU/COVID peptide vaccination (VaxigripTetra Quadrivalent Flu vaccine and Biovacc-19 Peptides CV1-5, Table S1) and served as positive and negative controls for the ELISA method.

ELISA

NGVEGF peptide-specific antibodies were detected as follows. Briefly, streptavidin (Sigma, CAT N° SA101, Sweden) diluted with phosphate buffered saline (PBS) (Sigma, CAT N° SA9418, Sweden) was coated onto micro plates (Nunc AS, CAT N° 442404, Denmark) at a concentration of 10 ng per well and incubated for 2 h at 37°C. Wells were then coated with the spike peptide NGVEGF (H-PCNGVEGFNCYGGG(K(Biotin))-NH2, (Schafer-N, Copenhagen, Denmark), diluted in PBS with 1% bovine serum albumin (BSA) and 0.05% Tween-20 (Amresco, CAT N° 0777) to a concentration of 10 ng per well and incubated for 2 h at 37°C. For optimization of the assay, sera were diluted in various optimization experiments from 1:4, 1:8; 1:16; 1:32, 1:64 and 1:128 and we used spike peptides biotinylated in either the N or C terminal, with or without a cysteine bridge to assess antibody reactivity. As most people should have been exposed to influenza A H1N1 and H2N3 strains during the last decade, and flu specific antibodies can be passively transferred to infants via placenta before birth, optimal negative control sera are hence lacking, and we therefore relied on negative controls for peptide reactivity of irrelevant peptides for optimizing the ELISA test. We confirmed a lack of NGVEGF specific antibodies in mice plasma (Figure S2) and observed that flu vaccination elicited development of NGVEGF peptide specific IgM and IgG antibodies in mice (positive control Figures S2A and S2B). These sera served as negative and positive controls, respectively for the optimization/validation of the ELISA NGVEGF test. For NGVEGF peptides, we found an optimal binding to peptides with a cystein bridge and biotinylated in the N terminus.

During optimization of the method, we noted that antibody reactivity to linear NGVEGF-containing peptides was lower than to peptides with a cysteine bridge (containing its natural loop structure, see Figure 1A) or to peptides biotinylated in the C-terminal end of the peptide (Figure S3). We therefore chose to use a cysteine loop containing the NGVEGF peptide biotinylated in the N terminus for the ELISA test. An adenovirus peptide previously used as negative peptide served as negative control. Mice sera from unvaccinated and FLU vaccinated mice were used as positive and negative controls (see below). After optimization, we used the serum/plasma concentration of 1:32 in PBS containing 1% BSA to assess binding to the spike peptide biotinylated in the N terminus for detection of antibodies binding to the NGVEGF peptide, as described in the results section (for prevalence estimation). All tests were done in duplicates. The ELISA plates were washed three times with PBS and 0.05% Tween-20 after each incubation step. For detection of antibody binding to the peptides, the plates were incubated with alkaline phosphatase–conjugated anti-human IgG (1:3000, Merck, CAT N° AP113, RRID:AB_92435) for 1 h at 37°C and then with alkaline

phosphatase substrate (Sigma, CAT N° P7998). After 30 min of incubation at room temperature in the dark, the reaction was terminated by adding 3 mol/l NaOH (Substrate at Karolinska University Hospital). Absorbance at 405 nm (A405) was measured with a spectrophotometer (Versamax, Molecular Devices). Mean values of the absorbance value for the two dilutions were calculated.

EXPERIMENTAL MODEL AND SUBJECT DETAILS

In vivo mouse model to test NGVEGF peptide antibody response

Swiss-Webster female mice aged 6–8 weeks received the influenza Vaxigrip vaccine (n = 12) on day 1 of the experiment; while controls (n = 8) received saline injections. A boost with the Vaxigrip vaccine coated with five SARS-CoV-2 peptides (CV-1–CV-5 (Biovacc-19) was given on day 23 to determine if mice could develop antibodies to the NGVEGF peptide. Mice were maintained under controlled conditions throughout the experiment (ambient temperature of 22 ± 2°C, a 12-h light/dark cycle). The mice were housed 4 per cage and had free access to standard chow diet and water. The study protocol was approved by II Local Ethics Committee for Animal Experiments in Warsaw (Approval no. 16.07.2021). Six mice were anesthetized with isoflurane and decapitated 2 weeks after the first immunization and another six mice 4 weeks after the boost vaccination. Whole blood was collected into sterile Eppendorf tubes. The samples were allowed to clot for 1 h at 37°C, cooled to 4°C, and centrifuged twice at 10,000 x *g* for 10 min each. Supernatants (serum) were aspirated and stored at 4°C and used as positive and negative controls for the ELISA assay.

Vaccine preparation

For the prime vaccination, VaxigripTetra Quadrivalent Flu vaccine (Sanofi Pasteur) was thawed, diluted 1:199 in saline, and 50 μl was injected subcutaneously in the neck with an insulin syringe; controls were injected with 50 μl of saline. Mice were randomly assigned to the groups. For boosting, a solution of 500 μl of Vaxigip, 50 μl of CV-1–CV-5 SARS-CoV-2 peptides (Immunor AS; Table S1), and 50 μl of saline was prepared and incubated at 4°C for 3 days. On day 4, the solution was kept at room temperature for 8 h and frozen at −80°C for 24 h. On the day of injection, the vaccine solution was thawed, diluted 1:143 in saline, and immediately injected at a dose of 50 μl.

Serology with a suspension bead array

Protein and peptide bead arrays were prepared, and assays to test for SARS-CoV-2 positivity were done as described, with minor assay differences.[36] Briefly, color-coded magnetic microspheres (MagPlex, Luminex) were covalently coupled to SARS-CoV-2 proteins (Table S1). Neutravidin (neutravidin 31000, Thermo Scientific) was used to couple NGVEGF and NGVKGF biotinylated peptides of different lengths (Table S1) to assess for peptide specific antibodies. All microspheres were pooled and mixed with the serum samples diluted 1:50 in assay buffer (PBS supplemented with 3% BSA, 5% non-fat milk, and 0.05% Tween-20). After incubation for 1 h, bound immunoglobulins were fixed with 0.2% paraformaldehyde (43368, Alfa Aesar) and incubated with anti-human IgG conjugated to R-phycoerythrin (H10104, Invitrogen; 12-4998-82, eBioscience, RRID:AB_465926) for 30 min, followed by detection of spike proteins with a FlexMap3D (Luminex Corp, FLEXMAP-3D-RUO). The peptides were synthesized with a cysteine bridge and biotinylated at the N or C terminus, respectively. The highest reactivity was observed to the longer NGVKGF peptide biotinylated at the N terminus and containing the cysteine bridge, and was selected for further analyses.

The suspension bead array data was processed using R (3.6.1)[49] in RStudio (1.2.1335).[50] Raw fluorescent intensities were used for the proteins while the signals for the peptides (SARS-CoV-2, NGVEGF, NGVKGF and control peptides) were transformed per sample into number of median absolute deviations (MADs) around the sample median to control for sample specific background levels.[36] Seropositivity towards SARS-CoV-2 was determined as having reactivity towards two of three SARS-CoV-2 antigens (Table S1, two Spike and nucleocapsid C) as earlier described.[36]

Identification of IFN-γ producing T cells by flow cytometry (FACS)

Peripheral blood mononuclear cells (PBMCs) were isolated from blood samples with Lymphoprep (Stem Cell Technologies, CAT N° 7801),[51] and reactivity of CD4 and CD8 T-cells against the SPIKE 1 NGVEGF peptide (Spike RBD pep 3; 20 aa unconjugated, Schafer-N, Denmark) was analyzed by flow cytometry assay. Briefly, 2× 10^6 PBMCs in U-bottom shaped FACS tubes were stimulated for 2 h with 1.6 μg of peptides and incubated overnight with brefeldin A (0.02 μg/μl; Sigma, CAT N° B6542) in U-bottom format FACS tubes with not completely closed lids laying slightly on one side in the stand at 37°C in 5% CO_2. Cells were washed with PBS (Gibco, CAT N° 14200067) and 1% BSA (Sigma, CAT N° 9418) and stained with mouse anti-human CD4 eFluor 450 (eBioscience, CAT N° 48-0048-41, RRID:AB_2016607) or mouse anti-human CD8 PE (BD Biosciences, CAT N°555635, RRID:AB_395997). After incubation for 30 min in the dark at 4°C, cells were fixed, permeabilized with Cell Fixation Cell Permeabilization Kit (Life Technologies, CAT N° GAS004) according to the manufacturer's instructions), and stained with FITC-conjugated anti-interferon (IFN)- γ (BD Biosciences, CAT N° 561057, RRID:AB_10562566) and analyzed by flow cytometry. Cells stimulated with staphylococcal enterotoxin B domain (0.2 μg; SEB, Sigma, CAT N° S4881) served as positive controls. Negative cells were stained with corresponding isotypes: mouse anti-human IgG2b kappa eFluor 450 (eBiosciences, CAT N° 48-4732-80, RRID:AB_1272023) and mouse anti-human IgG1 kappa phycoerythrin, (both from BD Biosciences, CAT N° 555751, RRID:AB_398613) and mouse anti-human IgG1 FITC-conjugated antibodies (BD Biosciences, CAT N° 554679, RRID:AB_395505). Cells were analyzed by flowcytometry (Novocyte, AH Diagnostics). The specific stimulated cells positive for IFN-γ were gated and the same gating was used for the relevant isotype controls. Dead cells (propidium jodid

stained)(Thermofisher, CAT N° BMS500PI) were excluded in the gating. The percentage of gated IFN- γ positive cells in the isotype controls was subtracted from the gated specific stimulation.

COVID-19 suspension immunoassay (SIA)

The COVID-19 suspension immunoassay (SIA) was performed as described in[52] to assess for the presence of Spike 1 specific antibodies in subjects before and after flu and COVID-19 vaccination. Briefly, the recombinant spike 1 (S1) antigen (40591-V08H, amino acids (aa) 16-685, Sino Biological, Beijing, China) was coupled to 2.5 × 10^6 carboxylated differentially color-marked magnetic beads (MagPlex microspheres, Luminex Corp., Austin, Texas, US) using sulfo-N-hydroxysulfosuccinimide (sulfo-NHS) (ThermoFisher Scientific, Waltham, MA, USA) and 1-ethyl-3-[3 dimethylaminopropyl]carbodiimide hydrochloride (EDC) (Sigma Aldrich, Merck, Darmstedt, Germany), according to the manufacturer's instructions. For SARS-CoV-2 specific IgG determination, serum diluted 1:25 (2 μl serum and 48 μl buffer) in PBSTT (phosphate-buffered saline supplemented with 0.5% Tween 20 and Tris (50 mM, Sigma CAT N° GE17-1321-01) was added to 96-well microtiter plates. Vortexed and sonicated microsphere mixture (50 μl, 25 beads/μl PBSTT) was added to each well, giving a final serum dilution of 1:50. Subsequently, the plate was incubated for 60 min in the dark at room temperature on a plate shaker (400 rpm). Microspheres were then washed with 100 μl PBS, followed by addition of 100 μl (2 μg/ml PBSTT) biotinylated protein G (Pierce Biotechnology, ThermoFisher Scientific, Waltham, MA, USA), 30 min incubation, and washing. One hundred microliters (2 μg/ml PBSTT) streptavidin–phycoerythrin (SA-PE) (Invitrogen, ThermoFisher Scientific, Waltham, MA, USA) was then added, followed by an incubation period of 15 min. Finally, the microspheres were washed once before re-suspension in 100 μl PBS and analysis of 50 μl in a Luminex MagPix instrument (Luminex Corp., Austin, TX, USA). The assay cut-off for positivity was calculated as the average median fluorescence intensity (MFI) plus 6 SD plus 10% of 200 SARS-CoV-2 antibody-negative sera.

SARS-CoV-2 surrogate virus neutralization test (sVNT)

We tested the neutralizing capacity of antibodies in these plasmas in a virus neutralization cell culture test, but the plasma samples collected from the subjects before and after vaccination were toxic to the cultured cells and resulted in high cell death. This phenomenon was not observed when control sera were tested in the same assay; i.e. this was a plasma mediated toxicity in this assay, which was not observed in experiments using sera. As the plasmas were not possible to use in this cell culture assay aiming to test if antibodies had an inhibitory effect on SARS-CoV-2 infection, we used a SARS-CoV-2 surrogate virus neutralization test (sVNT).

Briefly, recombinant SARS-CoV-2 S1 protein (40591-V08H, amino acids (aa) 16-685, Sino Biological, Beijing, China) was coupled to 2.5 x 10^6 carboxylated differentially color-marked magnetic beads (MagPlex microspheres, Luminex) as described above for the COVID-19 SIA. Twenty-five microliter of biotinylated human angiotensin converting enzyme 2 (hACE2) (20 ng; 10108-H02H-B, Sino Biological, Beijing, China) and 5 μl plasma sample (in 20 μl PBSTT) were incubated for 45 min with 50 μl vortexed and sonicated SARS-CoV-2 S1-coupled beads (25 beads/μl PBSTT), giving a final serum dilution of 1/20. Subsequently, the suspension was washed with 100 μl PBS, followed by addition of 100 μl (2 μg/ml in PBSTT) SA-PE (Invitrogen, ThermoFisher Scientific, Waltham, MA, USA), a 15 min incubation, another PBS wash, addition of 100 μl PBS, and briefly mixing the final reactions on a plate shaker. The MFI was determined as described above for the COVID-19 SIA. All incubations were performed in the dark at room temperature and on a plate shaker (400 rpm). We noted that freeze thawing of the plasma samples significantly reduced binding inhibition, wherefore data was collected from samples only thawed only once. PBSTT served as a negative control. Percentage binding inhibition (% BI) for each sample was calculated using the following formula: % BI = (1 – (sample MFI/negative control MFI)) x 100.

Mathematical modeling

Preprocessing of time series data for Sweden

We here provide additional details related to the modeling presented in Figure 5. We used case data from Stockholm from the second wave only (Figures 5A–5D), since testing was not reliable during the first wave and later waves occurred due to the emergence of new variants. In particular, data from the Swedish Public Health Agency allowed for separation of cases by the original Wuhan strain versus the alpha strain spreading mainly during the third wave in Sweden. We use Stockholm County (as opposed to data from the whole nation), since Sweden is sparsely populated and geographical effects need to be taken into account when modeling on a national scale. Stockholm, on the other hand, is a densely populated small area with about 2.4 million inhabitants. We obtained the incidence data from the Swedish Public Health Agency, and then readjusted it to account for underreporting. Based on sero-prevalence data (also from the Swedish Public Health Agency), the seroprevalence was 10% in Stockholm at the start of the second wave (early September 2020) and rose to 22.6% in mid-February 2021, between the second and third waves.[13,14] These findings are consistent with the seroprevalence estimated from our own serology data estimated among blood donors to 16.2% (n = 328) in October 2020 and to 21.1% (n = 450) in late February 2021. Thus, the graphs displaying the incidence in Stockholm (blue curve in Figures 5A–5D) has been re-scaled with a factor of 2.4, chosen so that the total amount of cases match the sero-prevalence measurements reported above. Moreover, the cases caused by the alpha strain has been removed from the tail of the curve, starting January 2021, when total amount of cases began to rise again. We remark that we were also able to accurately model the third wave by incorporating alpha into the model, the details of which is published in.[13,14]

Choice of R_o-values

Relying on EpiEstim we estimated R_o for Stockholm to be 1.4 in September 2020. However, in mid-October the number of cases suddenly increase sharply, which either indicates a sudden increase in R_o, or possibly that the estimate 1.4 is a bit off due to reporting irregularities. With an R_o-value of 1.5 we get a good overall fit of the model and measured data throughout the growth phase September-October 2020. Therefore, we argue that the correct R_o-value is somewhere in the range 1.4-1.5, and in order to avoid misrepresenting the performance of Age-Act SEIR, we display the result of running it first with 1.4 and then with 1.5, the result of which is seen in Figures 4A and 4B, respectively.

Preprocessing of time series data for India

The time series for India was downloaded from the Johns Hopkins University (same data series as used by e.g. ourworldindata). To adjust for underreporting, we used seroprevalence data released by the Indian Council of Medical Research; 0.7 in May/June 2020, 7.1% in August/September 2020, 24.1% around January 1, 2021, and 67.6% in June/July 2021. Up until this measurement, the cumulative number of registered cases was around 3%, indicating a massive underreporting. We used an underreporting factor of nearly 32 (i.e. 32 actual cases per registered case), chosen to match the 67.6 measurement, and rescaled the data series accordingly. This gives around 0.4, 10 and 23% cumulative number of cases on the earlier reported measurement times, which coincides well with measured data. Also, a measurement from early November 2021 among unvaccinated children indicated that 80% had had the virus, and with our underreporting factor the corresponding value in the time series was 77%. In summary, we argue that the time series, rescaled as described above, fits well with reported sero-prevalence measurements throughout the modeling time frame, and hence that this data series can be taken as a reliable input to compare with. The above mentioned values have been reported widely, see e.g. (https://www.bmj.com/content/374/bmj.n1856 https://www.icmr.gov.in/pdf/press_realease_files/Newsletter_English_July_2021.pdf https://www.hindustantimes.com/india-news/6th-delhi-sero-survey-shows-97-prevalence-101635443569509.html)

Concerning modeling details, we used the Age-Act stratified SEIR developed by Britton et. al that we updated to be able to model various strains simultaneously, along the same lines as described carefully in.[13,14] The code used is available on https://github.com/Marcus-Carlsson/Covid-modeling, and contains further details about particular parameter choices.

QUANTIFICATION AND STATISTICAL ANALYSIS

Unpaired t test was used to analyze the levels of IgG antibodies toward the same peptides in two different cohorts and ratio paired t test was used to analyze the differences between the pairs for the levels of IgG antibodies toward different peptides in the same cohort. One-way ANOVA followed by Turkey's multiple comparison test was used for multiple comparisons to analyze median absolute deviations (MAD) for two different peptides (NGVEGF and NGVKGF) for COVID-19-positive and COVID-19-negative cohorts. Paired t test was used to analyze the MAD values for one peptide (LKPFERDIS) for COVID-19-positive and COVID-19-negative cohorts. Unpaired t-test was used to analyze MAD values for different peptides in two different cohorts. Paired t test was used to analyze the same cohorts before and after vaccinations. Data are presented as mean +SEM. All statistical analyses were done with GraphPad Prism 9.